Tribbles pseudokinase 3 drives cancer stemness in oral squamous cell carcinoma cells by supporting the expression levels of SOX2 and EGFR

YU-HAO HUANG[1], PENG-JU CHIEN[1], WEN-LING WANG[1], LI-SUNG HSU[2],
YEN-MIN HUANG[3-5] and WEN-WEI CHANG[1,6]

[1]Department of Biomedical Sciences, Chung Shan Medical University, Taichung 402306, Taiwan, R.O.C.; [2]Institute of Medicine, Chung Shan Medical University, Taichung 402306, Taiwan, R.O.C.; [3]Division of Hematology and Oncology, Department of Internal Medicine, Keelung Chang Gung Memorial Hospital, Chang Gung Medical Foundation, Keelung 204201, Taiwan, R.O.C.; [4]Hemophilia and Thrombosis Treatment Center, Keelung Chang Gung Memorial Hospital, Chang Gung Medical Foundation, Keelung 204201, Taiwan, R.O.C.; [5]School of Medicine, College of Medicine, Chang Gung University, Taoyuan 333323, Taiwan, R.O.C.; [6]Department of Medical Research, Chung Shan Medical University Hospital, Taichung 402306, Taiwan, R.O.C.

Abstract. Oral squamous cell carcinoma (OSCC) is a type of head and neck cancer (HNC) with a high recurrence rate, which has been reported to be associated with the presence of cancer stem cells (CSCs). Tribbles pseudokinase 3 (TRIB3) is involved in intracellular signaling and the aim of the present study was to investigate the role of TRIB3 in the maintenance of CSCs. Analysis of The Cancer Genome Atlas database samples demonstrated a positive correlation between TRIB3 expression levels and shorter overall survival rates in patients with HNC. Knockdown of TRIB3 in the SAS and HSC-3 OSCC cell lines reduced cell proliferation through the induction of cell cycle arrest, but not of apoptosis. The population of OSCC-CSCs, defined by a high level of intracellular aldehyde dehydrogenase activity and the ability to form tumorspheres, was also reduced in TRIB3-silenced OSCC cells. The tumorigenicity of tumorspheres derived from the SAS OSCC cell line was reduced following TRIB3 knockdown. These results suggested the potential involvement of TRIB3 in the self-renewal capability of the OSCC CSCs. Mechanistically, TRIB3 was shown to positively regulate SOX2 expression via maintaining both the protein expression level and the SOX2 promoter-binding capability of E2F transcription factor 1 (E2F1). Additionally, TRIB3 also increased the expression level of EGFR through preventing its lysosomal degradation. The significant associations between TRIB3 and E2F1, SOX2 or EGFR expression were also confirmed using a HNC tissue array. Taken together, the findings of the present study may suggest that TRIB3 is an oncogenic protein that supports the stemness of OSCC and that targeting TRIB3 may be a potential strategy for OSCC therapy in the future.

Correspondence to: Dr Yen-Min Huang, Division of Hematology and Oncology, Department of Internal Medicine, Keelung Chang Gung Memorial Hospital, Chang Gung Medical Foundation, 222 Maijin Road, Anle, Keelung 204201, Taiwan, R.O.C.
E-mail: hym1000@gmail.com

Dr Wen-Wei Chang, Department of Biomedical Sciences, Chung Shan Medical University, 110 Section 1 Chien-Kuo North Road, Taichung 402306, Taiwan, R.O.C.
E-mail: changww@csmu.edu.tw

Introduction

Oral squamous cell carcinoma (OSCC) is the most common type of head and neck cancer (HNC), which accounts for ~90% of HNC cases and its incidence varies depending on the geographic region, patient age and lifestyle factors (1). The causes of OSCC include genetic alterations in several genes, including p53, PIK3 catalytic subunit a and Myc (2), and environmental factors, including tobacco use, alcohol consumption and betel quid chewing (3). The treatment of OSCC usually comprises surgery, radiation therapy, chemotherapy or immunotherapy, although the effectiveness of these treatments is ultimately limited due to factors such as late-stage diagnosis, tumor heterogeneity, development of drug resistance and high rates of recurrence and metastasis. The 5-year survival rate for patients with OSCC remains relatively low, at ~50% (4). Understanding the underlying molecular mechanisms that govern OSCC development and progression should assist in the design of more effective targeted therapies. Cancer stem cells (CSCs) have been identified as a critical population of

cancer cells for the development and progression of OSCC. OSCC-CSCs may be identified according to the positive expression of CD44 (5) or a high activity level of intracellular aldehyde dehydrogenase (ALDH) (6). This particular cancer cell type has been found to be strongly associated with tumor metastasis and resistance to chemotherapy or radiotherapy (7). Therefore, targeting CSCs may be an effective strategy for treating OSCC to improve patient outcomes (8). Tribbles pseudokinase 3 (TRIB3) is a member of the Tribbles family of proteins that is characterized by three structural domains: An N-terminal domain that participates in cellular localization, a pseudokinase domain (PKD) involved in protein-protein interactions and a C-terminal domain that is implicated in its ubiquitination (9). TRIB3 interacts with various proteins involved in cellular processes and it serves a critical role in the regulation of downstream signaling pathways, including the PI3K/Akt/mTOR (10), NF-κB (11) and MAPK/ERK pathways (12). The role of TRIB3 in cancer malignancy, however, currently remains unknown. ABTL0812, a novel autophagy inducer, has been used in clinical trials for the treatment of various cancer types, such as colorectal cancer, endometrial cancer and non-small cell lung carcinoma (13), where TRIB3 has been proposed as a key molecule to suppress the Akt/mTOR pathway to achieve anticancer effects (14). Qu et al (15) reported that overexpression of TRIB3 in endometrial cancer (EC) cells inhibited Akt activation and induced apoptosis. By contrast, our previous study reported that knockdown of TRIB3 in EC cells suppressed β-catenin activation and inhibited the self-renewal capability of EC-CSCs (16). Subsequently, Shen et al (17) demonstrated that overexpression of TRIB3 promoted cell proliferation in OSCCs by activating the Akt/mTOR pathway.

While previous studies have established the role of TRIB3 in various types of cancer, including OSCC, the present study aimed to focus on its specific involvement in maintaining CSC properties in OSCC. By employing bioinformatics analysis and a series of in vitro experiments, the present study aimed to demonstrate that TRIB3 acted as an oncogenic protein that supported the stemness characteristics of OSCC cells. Uncovering the novel molecular mechanisms involving TRIB3 not only advances the understanding of OSCC pathogenesis but could also identify new potential therapeutic targets for OSCC treatment.

Materials and methods

Analysis of the head and neck squamous cell carcinomas (HNSC) dataset of the cancer genome atlas (TCGA) database. The differential expression of TRIB3 mRNA between normal and HNSC tissues was analyzed using the Gene Expression Profiling Interactive Analysis 2 web server (GEPIA2; http://gepia2.cancer-pku.cn/#index). RNA-sequencing (RNA-seq) data from paired normal and tumor tissues of 19 patients with HNSC were downloaded from the Cancer Genomics Hub (https://cghub.ucsc.edu) and analyzed using GraphPad Prism software (version 5.0; Dotmatics). Overall survival data from the HNSC dataset in the TCGA database were downloaded from the Oncolnc web server (http://www.oncolnc.org/) and analyzed using GraphPad Prism software (version 5.0; Dotmatics).

Cell lines and culture conditions. The SAS (RRID: CVCL_1675) and OECM1 (RRID: CVCL_6782) OSCC cell lines were obtained from Professor Cherng-Chia Yu at the Institute of Oral Sciences in Chung Shan Medical University (Taichung, Taiwan). The HSC-3 cell line (RRID: CVCL_1288) was purchased from MilliporeSigma. All OSCC cell lines were cultured in DMEM (Thermo Fisher Scientific, Inc.) supplemented with 10% FBS (HyClone; Cytiva), 1 mM glutamine (Gibco; Thermo Fisher Scientific, Inc.), 100 μg/ml penicillin/streptomycin/amphotericin B (Gibco; Thermo Fisher Scientific, Inc.) and 1 mM sodium pyruvate (Gibco; Thermo Fisher Scientific, Inc.). The authentication of the cell lines was performed by short tandem repeat analysis at the Center for Genomic Medicine, National Cheng Kung University (Tainan, Taiwan). All cell lines were tested for mycoplasma contamination using the MycoAlert™ PLUS Mycoplasma Detection Kit (cat. no. LT07-710; Lonza Group, Ltd.) and were confirmed to be mycoplasma-free.

Gene silencing. Lentiviral-delivered shRNA was used for gene silencing, with shRNA targeting LacZ (shLacZ) serving as a negative control. The production and transduction of lentiviruses carrying TRIB3-, SOX2- or LacZ-specific shRNAs were performed according to our previous report (16). The shRNA plasmids were provided by the RNA Technology Platform and Gene Manipulation Core Facility (RNAi core) of the National Core Facility for Biopharmaceuticals at Academia Sinica in Taiwan as follows: Plasmids pCMVΔ8.91, pMD.G and gene-specific shRNAs [TRIB3 #1 (cat. no. TRCN0000307989), TRIB3 #2 (cat. no. TRCN0000295920), SOX2 #1 (cat. no. TRCN0000257314), SOX2 #2 (cat. no. TRCN0000355638) and LacZ (cat. no. TRCN0000231722)]. The 293T cells were obtained from the Bioresource Collection and Research Centre (BCRC) in accordance with the recommended protocol from RNAi Core. A plasmid DNA mixture (2.5 μg shRNA, 2.25 μg pCMVΔ8.91 and 0.25 μg pMD.G) was complexed with NTRII DNA transfection reagent (cat. no. JT97-N002M; T-Pro Biotechnology) at a ratio of 1 μg DNA:3 μl transfection reagent in OptiMEM media (Thermo Fisher Scientific, Inc.) at room temperature for 15 min. Subsequently, DNA/transfection reagent complexes were added to 293T cells and incubated at 37°C for 8 h. Following this, the culture media was replaced with fresh media (DMEM containing 10% FBS and 1.1 g/100 ml BSA). Media containing lentivirus particles were collected at 48 h post-transfection by removing 293T cells with centrifugation at 300 x g at room temperature for 5 min. Following filtration through a 0.45 μm filter, the media were used for titration of lentivirus titer by transduction to A549 cells (BCRC) with a serial of medium volume followed puromycin selection and cell viability test. Lentivirus-containing media were then utilized to transduce OSCC cells at 30% confluence in a multiplicity of infection (MOI) of 1 with 8 μg/ml polybrene (MilliporeSigma) at 37°C for 24 h. Thereafter, the medium was replaced with fresh medium containing 2 μg/ml puromycin (TOKU-E Corporation) to select successfully transduced cells at 37°C for 48 h. The shRNA sequences used were as follows: TRIB3#1, 5'-CCGGGCTAGTTCTTGTCT AACTCAACTCGAGTTGAGTTAGACAAGAACTAGCTT TTTG-3'; TRIB3#2,5'-CCGGGCCGTGCTCTTCCGCCA GATGCTCGAGCATCTGGCGGAAGAGCACGGCTTTTTG3';

SOX2#1,5'-CCGGTGGACAGTTACGCGCACATGACT CGAGTCATGTGCGCGTAACTGTCCATTTTTG-3'; SOX2 2,5'-CCGGCCCTGCAGTACAACTCCATGACTCGAGTC ATGGAGTTGTACTGCAGGGTTTTTG-3'; and LacZ, 5'-CCGGCGCGATCGTAATCACCCGAGTCTCGAGAC TCGGGTGATTACGATCGCGTTTTTG-3'.

TRIB3 knockdown was also achieved by transfecting cells with siRNA oligos. Briefly, cells at 30-40% confluence were transfected with siRNAs (0.35 µg) using the TransIT-X2™ Dynamic Delivery System (cat no. MIR 6000; Mirus Bio, LLC). A negative control (siNC; Life Technologies) and a TRIB3-specific siRNA mixture (siTRIB3; cat. no. sc-44426; Santa Cruz Biotechnology, Inc.) were used. After 48 h of incubation at 37˚C, the cells were harvested for further experiments. The TRIB3 siRNA mixture contained three siRNA duplexes with the following sequences: A sense, 5'-GACAAA CUGGCAUCCUUGATT-3' and antisense, 5'-UCAAGGAUG CCAGUUUGUCTT-3'; B sense, 5'-GGAUACCAUGAGUAU GUAUTT-3' and antisense, 5'-AUACAUACUCAUGGUAUC CTT-3'; C sense, 5'-GUUUACCUGUGCCUAAUAATT-3' and antisense, 5'-UUAUUAGGCACAGGUAAACTT-3'; and siNC sense, 5'-ACGUGACACGUUCGGAGAAUU-3' and antisense, 5'-AAUUCUCCGAACGUGUCACGU-3'.

Senescence-associated heterochromatin foci (SAHF) staining with Hoechst 33342. Cells ($5x10^4$ cells/well) were seeded into 12-well plates. Subsequently, cells were transduced with shLacZ or shTRIB3 as previously described, or treated with 100 µM H_2O_2 at 37˚C for 30 min. After 48 h, cells were fixed with 4% paraformaldehyde for 15 min at room temperature. Cellular DNA was stained with 50 µg/ml Hoechst 33342 at room temperature for 10-15 min. An LSM900 confocal microscope (Zeiss AG) was used to capture images of Hoechst-stained nuclei and to visualise the Hoechst puncta indicative of SAHF using ZEN microscopy software (version 3.7, ZEISS).

Gene overexpression by transient transfection. Cells ($1x10^5$ cells/well) were seeded into 6-well plates and incubated until 30-40% confluency prior to transfection. Transfections were performed using the TransIT-X2™ Dynamic Delivery System according to the manufacturer's protocol. Plasmid DNA of the pCMV3 untagged negative control vector (pCMV3-NCV) or full length TRIB3 plasmid (pCMV3-TRIB3-flag) was mixed with TransIT-X2 reagent at a ratio of 1 µg DNA:3 µl reagent at room temperature for 15 min and then added to cells. Cells were incubated at 37˚C for 48 h. After transfection, cells were harvested using 0.05% trypsin containing 0.53 mM EDTA (cat. no. 15400054; Thermo Fisher Scientific, Inc.) at room temperature for 3 min and subsequently processed for experimental analysis.

Tumorsphere cultivation. Tumorsphere cultivation was conducted as per our previous study (15). Briefly, single cell suspensions of OSCC cells were suspended in culture medium [(DMEM/F12 media (Thermo Fisher Scientific, Inc.) containing 0.4% BSA (MilliporeSigma), 1X B27 supplement (Gibco; Thermo Fisher Scientific, Inc.), 20 ng/ml EGF (PeproTech, Inc.), 20 ng/ml basic FGF (PeproTech, Inc.), 5 µg/ml insulin (MilliporeSigma), 1 µg/ml hydrocortisone (MilliporeSigma) and 4 µg/ml heparin (MilliporeSigma)]. The

cell suspensions were seeded into ultralow attachment 6-well plates (Greiner Bio-One Ltd.) and incubated at 37˚C in a 5% CO_2 incubator for 7 days. For primary tumorsphere culture, a density of $1x10^4$ cells/well was used. For secondary tumorsphere formation, the primary tumorspheres were collected using 100 µm cell strainers (BD Biosciences), dissociated into single cells by incubating with HyQTase (MilliporeSigma) and seeded at a density of $5x10^3$ cells/well. To examine the role of E2F1 in tumorsphere forming capability, a pan E2F inhibitor, HLM006474 (cat. no. S8963; Selleck Chemicals) was added to the tumorsphere culture media at a final concentration of 40 µM, followed by incubation at 37˚C for 7 days.

Clonogenic assay. SAS and HSC3 OSCC cells after transducing with shRNA carrying lentiviruses were plated at a density of 200 cells/well in 12-well plates and incubated at 37˚C for 7-10 days. After fixation with 2% formaldehyde at room temperature for 5 min, the cell colonies were stained with 1% crystal violet (MilliporeSigma) for 1 h at room temperature and the number of colonies, defined as consisting of ≥50 cells, were imaged using an inverted light microscope (AE30; Motic Incorporation, Ltd.) and counted manually.

ALDEFLUOR assay using FACS. Following transduction of the SAS cells with shRNA lentiviruses, the population of ALDH+ cells was using the ALDEFLUOR assay (cat. no. 01700; Stemcell Technologies, Inc.), in accordance with the manufacturer's protocol. To establish a negative control for gating the ALDH+ cell population, a subset of cells was treated with 15 µM diethylaminobenzaldehyde (DEAB), a specific ALDH inhibitor. Fluorescence signals were measured using a FACSCanto™ II flow cytometer (BD Biosciences) with FASCDiva software (version 8.0; BD Biosciences) and analyzed using FlowJo software (version 10; BD Biosciences). The ALDH+ cells were defined by setting the gate such that the DEAB-treated samples showed <1% positive cells.

Western blotting and co-immunoprecipitation (co-IP). Western blotting and co-IP analyses were conducted as per our previous study (16). Whole cell lysates of OSCC cells were prepared by cell lysis in RIPA buffer (25 mM Tris-HCl pH 7.6, 150 mM NaCl, 1% NP-40, 1% sodium deoxycholate and 0.1% SDS). For western blotting, 25 µg of total proteins per lane were loaded into 10% SDS-PAGE gel for protein separation by electrophoresis. Subsequently, the separated proteins were transferred onto 0.45 µm PVDF membranes (cat. no. 66547; Pall Corporation). After blocking with nonfat dry milk 5% w/v in TBS buffer (cat. no. GTX48889; GeneTex, Inc.) at room temperature for 1 h, the membranes were then incubated with primary antibodies at 4˚C for 16 h (Table SI). After washing with 0.1% Tween-20/TBS buffer, the membranes were incubated with secondary antibodies for 1 h at room temperature, followed by incubation with horseradish peroxidase-conjugated secondary antibodies at room temperature for 1 h. The signal was then developed using Pierce ECL Western Blotting Substrate (Thermo Fisher Scientific, Inc.) and imaged using the Amersham Imager 680 (Cytiva). For co-IP analysis, 1 mg of total cellular proteins were added into IP buffer (20 mM HEPES pH 7.9, 2 mM $MgCl_2$, 0.2 mM EDTA, 0.1 mM KCl, 1 mM dithiothreitol, 10% glycerol and 0.1% NP-40) followed

by the addition of the appropriate antibodies and subsequent incubation at 4°C overnight. The protein complexes were further isolated using Protein G Mag Sepharose (cat. no. 28944008, Cytiva) followed by western blotting analysis as described above. Band intensities were quantified using Image J software (version 1.54k; National Institutes of Health).

Cell cycle analysis using 5-bromo-2-deoxyuridine (BrdU). Cell cycle analysis was performed using the FITC BrdU Flow Kit (cat. no. 559619; BD Pharmingen; BD Biosciences) according to the manufacturer's instructions. Briefly, BrdU was added to cell culture media at a final concentration of 10 μM and incubated at 37°C for 2 h before harvesting cells using trypsin/EDTA (cat. no. 15400054; Thermo Fisher Scientific, Inc.). The harvested cells were then fixed with the fixation buffer provided in the kit at room temperature for 30 min. After washing with washing buffer provided in the kit and centrifugation at 4°C at 300 x g for 10 min, cells were then resuspended in permeabilization buffer containing FITC-conjugated anti-BrdU antibodies, which were supplied in the FITC BrdU Flow Kit, as a dilution of 1:50 at room temperature for 1 h followed by staining with 7-AAD at 4°C protected from light for 30 min. The fluorescence signals of FITC and 7-AAD were measured using FACS Canto-II flow cytometry (BD Biosciences). Cell cycle distribution was analyzed using FlowJo software (version 10.8.0; FlowJo LLC; BD Biosciences).

Chromatin immunoprecipitation (ChIP). ChIP analysis was performed according to the protocol described in our previous report (15). The presence of the SOX2 promoter sequence within the precipitated DNA was detected using SYBR Green-based quantitative PCR (qPCR) with the iTaq Universal SYBR Green Supermix (Bio-Rad Laboratories, Inc.). The primer sequences used were as follows: SOX2-CoreP-E2F1-site1 forward (F), 5'-GAGAAGGGCGTGAGAGAGTG-3' and reverse (R), 5'-AAACAGCCAGTGCAGGAGTT-3'; and SOX2-CoreP-E2F1-site2 F, 5'-TGGAAGCAAGGAAGGTTTTG-3' and R, 5'-GTCATTGTTCTCCCGCTCAT-3'. The thermocycling conditions used were as follows: 95°C for 3 min; followed by 40 cycles of 95°C for 10 sec and 60°C for 60 sec. The data were analyzed using the percent input method, which calculates levels relative to input chromatin, as previously recommended (18).

Immunofluorescence analysis and imaging. Cells were washed with PBS buffer followed by fixation with 4% paraformaldehyde at room temperature for 15 min and permeabilization with 0.1% Triton X-100 at room temperature for 10 min. After blocking with 1% BSA/PBS at room temperature for 1 h, primary antibodies were added and incubated with the cells at 4°C overnight. The cells were then incubated with fluorescein-conjugated secondary antibodies at room temperature for 1 h in the dark. The cells were imaged using a ZEISS LSM 510 Meta confocal microscope (Zeiss AG). The colocalization of fluorophores was analyzed using ImageJ software (version 1.54k; National Institutes of Health) with a Colocalization Finder plugin (http://questpharma.u-strasbg.fr/html/colocalization-finder.html) to calculate the Pearson's correlation coefficient of the two fluorophores.

E2F1 reporter assay. To investigate whether TRIB3 enhanced E2F1-induced transcriptional activity, luciferase-based reporter plasmids were constructed. These plasmids contained eight repeats of either the wild-type (wt) or mutant (mut) E2F1 binding DNA elements. The sequence for the wt element was 5'-TTTCGCGCCA-3' and the sequence for the mut element was 5'-TTGCTCGACC-3', as previously detailed by Iglesias-Ara *et al* (19). These sequences were designed to assess E2F-induced transcriptional activity. The E2F1 reporter plasmids were mixed with pRL plasmid DNA (cat. no. E223; Promega Corporation), which carried the Renilla luciferase gene to assess the transfection efficiency. The DNA/transfection reagent complex was formed by combining the plasmids with the TransIT-X2™ transfection reagent at a ratio of 1 μg DNA:3 μl reagent at room temperature for 30 min followed by adding into cell culture wells for 24 h. The cell lysates were harvested using passive lysis buffer (cat. no. E1941; Promega Corporation). Luciferase activity was measured using the Dual-Luciferase assay system (cat. no. E1910; Promega Corporation) and the GloMax® 20/20 Luminometer with the spectral range of light emission of 565±10 nm (Promega Corporation).

Prediction and examination of protein-protein interaction between TRIB3 and E2F1. The amino acid (a.a.) sequences of TRIB3 (accession no. NP_066981.2) and E2F1 (accession no. NP_005216.1) were retrieved from the National Center for Biotechnology Information (NCBI) database (https://www.ncbi.nlm.nih.gov/gene) and their 3D protein structures were predicted using the Iterative Threading ASSEmbly Refinement (I-TASSER) platform (20). The interactions between TRIB3 and E2F1 were predicted using the DOCK Proteins module of the ZDOCK Server. The interaction residues of the potential complex were then examined using the Protein-Protein Interaction Server (InterProSurf; https://curie.utmb.edu/prosurf.html). The interaction sites were visualized using PyMol (version 2.4.1_198; Schrodinger) with manually annotated interacting amino acid residues. The full-length coding sequences of TRIB3 (accession no. NM_021158.5) and E2F1 (accession no. NM_005225.3) were obtained from the NCBI database. The E2F1 gene was further divided into N-terminal (a.a. 1-251) and C-terminal (a.a. 252-437) segments. The TRIB3 gene was further subdivided into N-terminal (a.a. 1-180), C-terminal (a.a. 181-358) and psudeokinase domain (a.a. 72-315) segments. The DNA sequences of full-length TRIB3, and two segments of E2F1 were then synthesized (Genewiz, Inc.) and cloned into the pcDNA3.0-HA (Genewiz, Inc.) or pCMV3-6xHis (Genewiz, Inc.) vectors, respectively. The restriction sites were BamGI at the 5' end and EcoRI at the 3' end for cloning into the pcDNA3.0-HA vector, and KpnI at the 5' end and XbaI at the 3' end for cloning into the pCMV3-6xHis vector. In addition, deletion mutants of TRIB3 with deletion of a.a. 174-179, a.a. 236-240 or double deletion of a.a. 174-179 and a.a. 236-240 were synthesized and cloned into the pcDNA3.0-HA vector. Plasmids carrying sequences of TRIB3 or E2F1 segments were co-transfected into 293T cells at a 1:1 ratio using the TransIT-X2™ transfection reagent. 293T cells were seeded into wells of 6-well plates at a concentration of 1×10^5 cells/well. The plasmid DNA was introduced into the cells by mixing the DNA and transfection reagent at a ratio of 1 μg DNA:3 μl reagent at room temperature for 15 min.

Complexed DNA was added into the wells containing the attached 293T cells, which were then incubated at 37°C for 48 h. Subsequently, the cell lysate was harvested by trypsin/EDTA treatment at room temperature for 3 min, then cells were lysed with RIPA buffer at 4°C for 5 min and 1 mg of total proteins were subjected to IP with anti-hemagglutinin (HA) antibodies, followed by immunoblotting with anti-polyhistidine (His) antibodies, as aforementioned for co-IP.

RNA extraction and reverse transcription-qPCR (RT-qPCR). Total RNA was extracted from OSCC cells using TRIzol® Reagent (Invitrogen; Thermo Fisher Scientific, Inc.). A total of 1 μg of RNA was reverse-transcribed to cDNA using the RevertAid First Strand cDNA Synthesis Kit (Thermo Fisher Scientific, Inc.). RT-qPCR was performed using the PCRmax Eco 48 real-time PCR system (Cole-Parmer Instrument Company, Ltd.) and iQ™ SYBR® Green Supermix (Bio-Rad Laboratories, Inc.). The thermocycling conditions used were as follows: 95°C for 3 min; followed by 40 cycles of 95°C for 10 sec and 60°C for 60 sec. The following primer sequences were used: SOX2 forward (F), 5'-GCTACAGCATGATGC AGGACCA-3' and reverse (R), 5'-TCTGCGAGCTGGTCA TGGAGTT-3'; and glucuronidase β (GUSB) F, 5'-CTGTCA CCAAGAGCCAGTTCCT-3' and R, 5'-GGTTGAAGTCCT TCACCAGCAG-3'. GUSB has been previously validated for use as a reference gene in OSCC cell lines (21). The expression level of SOX2 was normalized to that of GUSB and the results were analyzed using the $2^{-\Delta\Delta Cq}$ method (22).

In vivo tumorigenicity assay. The animal experiment was approved by the Institutional Animal Care and Use Committee at Chung Shan Medical University (approval no. 2437; Taichung, Taiwan). To obtain CSCs, SAS cells were cultured to form tumorspheres, which were then digested by HyQTase to obtain a single-cell suspension, as aforementioned. These cells were transiently transduced with lentiviruses carrying shRNA sequences of shLacZ or shTRIB3#1 and selected by 2 mg/ml puromycin at 37°C for 48 h. CAnN.Cg-Foxn1nu/CrlNarl nude male mice (aged 6 weeks) with an average body weight of 17.9±0.2 g were purchased from The National Laboratory Animal Center (Taipei, Taiwan). A total of 4 mice were used to examine the effect of TRIB3 on tumorigenicity *in vivo*. For each mouse, shLacZ transduced SAS cells were injected in the dorsal-left interscapular area, while shTRIB3#1 transduced cells were injected into the dorsal-right interscapular area. The injection cell number and volume was 1×10^4 cells/100 μl Matrigel (BD Biosciences) at a concentration of 2 mg/ml per site and a total of 4 mice were used to assess tumor formation. The mice were housed in an environment that maintained 12 h of light and 12 h of dark, a temperature of 22-24°C and humidity at 50-60%. The mice ate and drank *ad libitum*. Tumor growth was monitored twice per week. The mice were sacrificed on day 30 after the cell injection, when the tumor volume of the shLacZ control group reached ≥1,000 mm³. Tumor volume was calculated using the following equation: Dxd²/2, where 'D' represented the length of the tumor and 'd' represented the width of the tumor. Animals were sacrificed in a CO_2 cage at a flow rate of 30-70% of the cage volume/min. The xenograft tumors were then excised for weighing and immunohistochemistry (IHC) analysis.

IHC analysis. A human HNC tissue microarray paraffin sections containing 70 samples were purchased from TissueArray.Com (cat. no. HN802d). The company ensured that all tissue samples were collected with the full informed consent of the donors. The use of HNC tissue was approved by the Chang Gung Medical Foundation Institutional Review Board (approval no. 202002207B0C501). Xenograft tumors were excised and fixed in 5 ml of formaldehyde neutral buffer solution (cat. no. 11-0705; MilliporeSigma) for 16 h at room temperature, dehydrated through graded ethanol, cleared in xylene and embedded in Paraplast Plus paraffin resin (cat. o. P3683; MilliporeSigma). The xenograft tumor tissue sections (5 μm) or tissue microarray slides were stained with primary antibodies using the VECTASTAIN® Elite® ABC Universal PLUS Kit (cat. no. PK-8200; Vector Laboratories, Inc.; Maravai LifeSciences). Antigen retrieval was performed by heating the samples in Antigen Unmasking Solution (cat. no. H-3301; Vector Laboratories, Inc.; Maravai LifeSciences) in a pressure cooker at 120°C for 1 min followed by washing with PBS at room temperature for 5 min. The endogenous peroxidase activity was inactivated by incubating with BLOXALL Blocking Solution at room temperature for 10 min. The slides were then incubated with 2.5% normal horse serum (Vector Laboratories, Inc.; Maravai LifeSciences) at room temperature for 20 min. After blocking, the slides were incubated with primary antibodies, which were diluted with 1% BSA (cat. no. 05470; MilliporeSigma) diluted with PBS buffer (cat. no. 10010001; Thermo Fisher Scientific Inc.) at 4°C for 16 h. Details of the primary antibodies used for IHC analysis, including catalog numbers, manufacturers and dilutions are provided in Table SI. After washing three times with PBS/0.1% Tween-20 for 3 min/wash at room temperature, the slides were then incubated with prediluted biotinylated horse anti-mouse/rabbit IgG secondary antibodies that were supplied in the aforementioned kit at room temperature for 1 h, followed by washing three times with PBS/0.1% Tween-20 for 3 min/wash at room temperature. Slides were then incubated with the VECTASTAIN Elite ABC Reagent at room temperature for 30 min. The signals were then developed by incubating with 3,3'-diaminobenzidine (Dako) at room temperature until desired stain intensity developed. The sections were counterstained with Harris hematoxylin (MilliporeSigma) at room temperature for 1 min, followed by dehydration through graded ethanol and mounting. Tissues were imaged using bright-field microscopy on a TissueFAXS PLUS system (TissueGnostics GmbH) and analyzed using StrataQuest software (version 7.0; TissueGnostics GmbH).

Statistical analysis. All experimental data were expressed as mean ± SD, except for tumor weights which were presented as mean ± SEM. Cell experiments were repeated three times independently, while xenograft experiments were performed twice. Statistical analyses were performed using GraphPad Prism (version 5.0; Dotmatics). The unpaired Student's t-test was used to compare quantitative data between two groups, except for the comparison of TRIB3 between normal-tumor pairs from the HNSC dataset of the TCGA database, where the paired Student's t-test was used. One-way ANOVA followed by the post-hoc Tukey's Honestly Significant Difference test was used for the statistical analysis when comparing >2 groups.
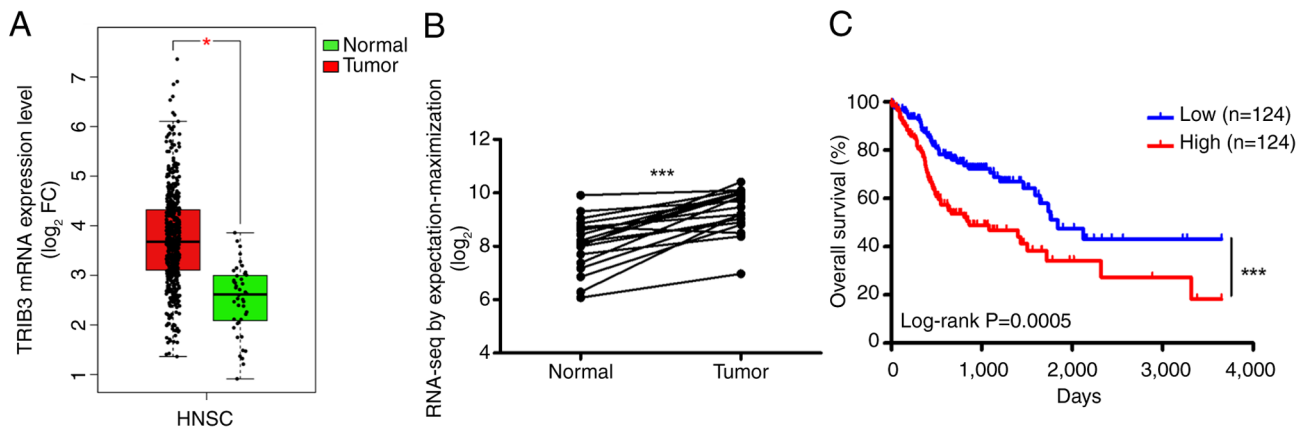
Figure 1. TRIB3 expression is positively correlated with the poorer overall survival in the TCGA HNC dataset. (A) The differential expression levels of TRIB3 mRNA in normal (green) and HNC (red) tissues were analyzed using the Gene Expression Profiling Interactive Analysis 2 website, a tool for analyzing TCGA RNA sequencing data (55). The expression data were first log2(TPM+1) transformed for differential analysis and presented as log2FC, which is defined as the median level of tumor samples-the median level of normal samples. Data were presented as mean ± SD. Tumor samples, n=519; normal samples, n=44, according to the information of TCGA database. (B) TRIB3 mRNA expression levels in 19 paired HNSC and normal tissues from the TCGA database were compared using the paired Student's t-test. (C) Overall survival curves for patients with HNSC with the highest 25% (n=124) and the lowest 25% (n=124) TRIB3 mRNA expression levels were analyzed using Kaplan Meier curves and the log-rank test. *P<0.05; ***P<0.001. TRIB3, tribbles pseudokinase 3; TCGA, The Cancer Genome Atlas; HNC, head and neck cancer; HNSC, head-neck squamous cell carcinoma.

Overall survival between high- and low-TRIB3 expression groups of patients with HNSC was calculated using the Kaplan-Meier method with a log-rank test. Correlations were analyzed using the Pearson correlation coefficient. P<0.05 was used to indicate a statistically significant difference.

Results

TRIB3 positively regulates cell proliferation in OSCC cells. The GEPIA2 tool was used to analyze the HNC RNA-seq dataset from the TCGA database, which demonstrated that the mRNA expression level of TRIB3 was significantly higher in HNC tissues compared with normal tissues (Fig. 1A). Additionally, in 19 pairs of matched HNC and normal tissue samples, TRIB3 mRNA expression was significantly higher in cancerous tissues compared with those in the adjacent normal tissues (Fig. 1B). Patients with HNC who showed the highest 25% expression levels of TRIB3 mRNA exhibited significantly lower overall survival rates compared with those in the lowest 25% expression levels of TRIB3 (Fig. 1C), suggesting that TRIB3 may function as a potential oncogene in HNC. Analysis of the western blotting results showed that the protein expression levels of TRIB3 in SAS cells were the highest, followed by HSC3 and OECM1 cells, respectively (Fig. S1). Subsequently, SAS and HSC3 cells were used for TRIB3 knockdown experiments with TRIB3-specific shRNA. These results showed a significant reduction in the numbers of cell colonies in shTRIB3-treated cells (Fig. 2A), suggesting the inhibition of cell proliferation after silencing TRIB3 expression. BrdU incorporation analysis demonstrated that knockdown of TRIB3 in SAS cells (Fig. 2B) or HSC3 cells (Fig. 2C) by TRIB3-specific siRNAs decreased the proportion of cells in S-phase and significantly increased the proportion of cells in G1-phase, although no increase was observed in the sub-G1 cell population. The dysregulation of cell cycle progression was also observed in shTRIB3 OSCC cells (Fig. S2). Cells treated with shTRIB3 demonstrated a

significantly reduced protein expression level of CDK6 in both SAS and HSC3 cells, compared with control cells (Fig. 2D). Other cell cycle-associated proteins, including cyclin A2, cyclin B1 and CDK1, showed a significant reduction in expression levels in OSCC cell lines transduced with one of the TRIB3-specific shRNAs, despite both shRNAs effectively knocking down TRIB3 protein expression (Fig. 2D). The decrease in expression levels of cyclin A2 and cyclin B1 were observed in SAS cells after transduction of shTRIB3#2, but not shTRIB3#1. Although the significant reductions of cyclin D1 were observed in SAS cells after transduction of both shRNAs, this effect was not observed in HSC3 cells (Fig. 2D). Furthermore, silencing of TRIB3 in SAS or HSC3 cells did not cause any upregulation of the protein expression level of cleaved caspase-3 (Fig. S3). These results suggested the presence of an apoptosis-independent mechanism of TRIB3 silencing in the decreased proliferation of OSCC cells that still led to cell cycle arrest. In addition, treatment of SAS or HSC3 cells with palbociclib, a small molecule inhibitor of CDK4/6 that is currently used for treating advanced or metastatic breast cancer (23), inhibited proliferation of cells in a dose-dependent manner (Fig. S4). In addition, the knockdown of TRIB3 in SAS cells caused cellular senescence as shown by the elevated senescence-associated heterochromatin foci (Fig. S5A). The increased level of H2AX at serine 139 in SAS cells after TRIB3 knockdown was observed, suggesting the induction of DNA damage (Fig. S5B). Taken together, these results suggested that TRIB3 contributed to regulation of the OSCC cell cycle and may be a potential therapeutic target for the treatment of OSCC.

Inhibition of TRIB3 expression decreases the self-renewal capability of OSCC-CSCs. Our previous study demonstrated that TRIB3 positively regulates the activity of CSCs in EC (16); therefore, the present study further investigated the effect of TRIB3 expression on the self-renewal capacity of OSCC-CSCs. Western blotting analysis demonstrated an increase
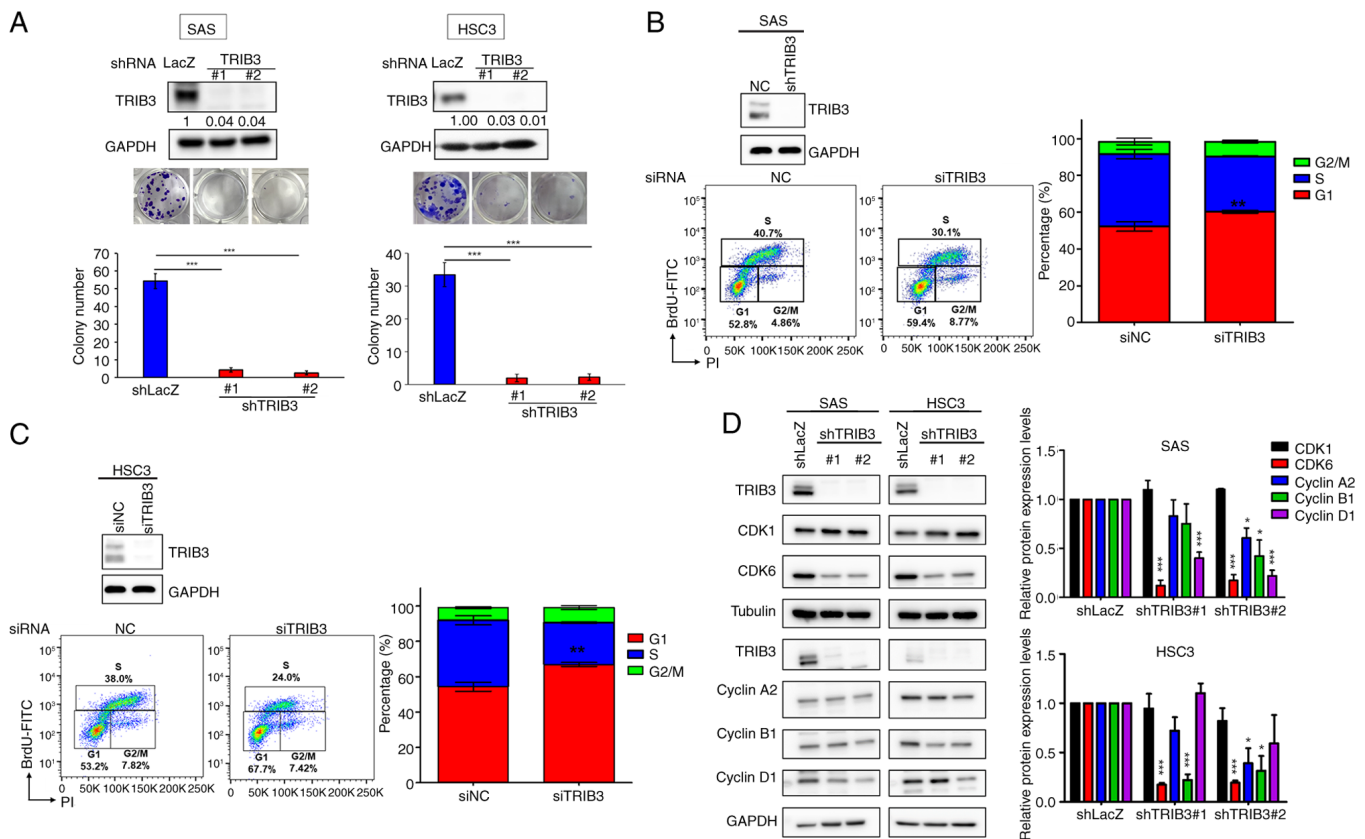
Figure 2. TRIB3 depletion decreases cell proliferation and affects cell cycle distribution. (A) SAS and HSC3 oral squamous cell carcinoma cells were transduced with lentiviruses carrying shRNA sequences for LacZ (control), sh-TRIB3#1 or sh-TRIB3#2. Western blotting results confirmed TRIB3 protein knockdown. Cell proliferation was assessed by clonogenic assay, with colonies stained using crystal violet and visualized on day 14. (B) SAS and (C) HSC3 cells were transfected with siRNA NC or siTRIB3 for 48 h. Cells were then harvested for western blotting analysis to verify TRIB3 protein depletion and for cell cycle analysis using BrdU. Anti-BrdU-FITC and PI fluorescence signals were detected using flow cytometry, analyzed using FlowJo software (version 10; FlowJo LLC; BD Biosciences) and quantified. Data represented the percentage of cells at each cycle phase and were presented as mean ± SD. (D) Western blotting analysis was used to determine the protein expression levels of cell cycle regulators Cyclin A2, Cyclin B1 and Cyclin D1 following TRIB3 shRNA transfection for 48 h in SAS and HSC3 cells. For quantification, CDK1 and CDK6 levels were normalized to Tubulin using the upper TRIB3 blot, while Cyclin A2, Cyclin B1 and Cyclin D1 levels were normalized to GAPDH using the lower TRIB3 blot. Blot images were representative of one of three independent experiments. Statistical analyses were conducted using one-way ANOVA with post-hoc Tukey's Honestly Significant Difference test. $^*P<0.05$; $^{**}P<0.01$; $^{***}P<0.001$. TRIB3, tribbles pseudokinase 3; shRNA, short hairpin RNA; siRNA, small interfering RNA; BrdU, 5-bromo-2-deoxyuridine; NC, negative control; si, siRNA.

in the protein expression level of TRIB3 in tumorspheres obtained from SAS or HSC3 cells (Fig. 3A). Furthermore, a reduced ALDH⁺ population of SAS cells was identified following TRIB3 knockdown (Fig. 3B). Inhibition of TRIB3 expression in SAS (Fig. 3C) or HSC3 cells (Fig. 3D) led to significant reductions in the formation of primary or secondary tumorspheres, showing that TRIB3 expression may serve an important role in the self-renewal capability of OSCC-CSCs. To further substantiate the role of TRIB3 in sustaining CSC activity in OSCC, CSCs from SAS cells were enriched through tumorsphere culture and their tumorigenicity was assessed in immunodeficient nude mice following lentiviral transduction with shTRIB3 or control shLacZ sequences (Fig. 3E). All mice remained alive at the day 28 and were to be sacrificed on day 30 after cell injection; however, 1 mouse was found deceased on day 30. Based on the post-mortem changes observed, which were similar with ~24 h decomposition time as previously reported (24), and as spontaneous mortality without previous signs of illness can be common in laboratory mice (25), the mouse likely died within 24 h before the scheduled sacrifice for unknown reasons. Tumor weights were quantitatively

analyzed and a significant reduction in the tumor weight of the shTRIB3 group (0.013±0.015 g) compared with that of the control shLacZ group (0.629±0.487 g) was demonstrated (Fig. 3F). Notably, while the shLacZ group showed variable tumor weights, the shTRIB3 group consistently produced small tumors (Table SII). This contrast in tumor weights may suggest a critical role for TRIB3 in maintaining the tumorigenic capacity of OSCC-CSCs. Considered together, these data suggest that TRIB3 may positively regulate the maintenance of OSCC-CSCs.

TRIB3 positively regulates SOX2 expression through an E2F1-mediated mechanism. To provide further support for the positive regulatory role of TRIB3 in the maintenance of OSCC CSCs, the expression levels of stem cell markers, including CD44 (26,27) and KRT19 (28,29), were examined by western-ting blot analysis. These results demonstrated that knockdown of TRIB3 led to a significant reduction in the levels of these CSC markers. However, silencing TRIB3 did not cause any upregulation of the expression of epithelial markers, such as E-cadherin (30) or KRT4 (31) (Fig. 4A). A significant reduction
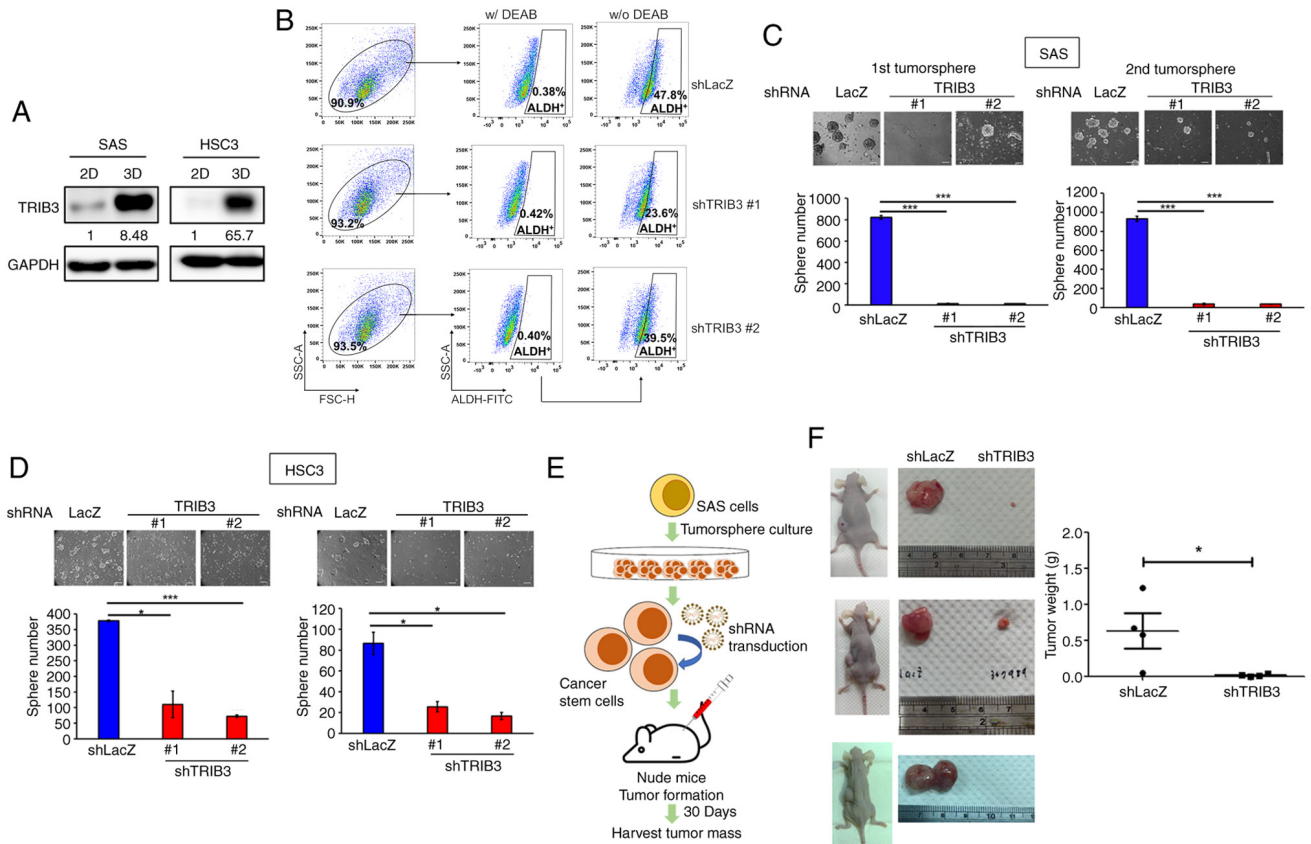
Figure 3. Knockdown of TRIB3 impairs the self-renewal capability of oral squamous cell carcinoma cells. (A) Western blotting analysis of TRIB3 protein expression levels in SAS and HSC3 cells cultured in conventional adherent conditions (2D) or as tumorspheres (3D). GAPDH served as the loading control. (B) ALDEFLUOR assay and flow cytometry quantification of ALDH⁺ cells in SAS cells transduced with lentiviruses carrying shLacZ, shTRIB3#1 or shTRIB3#2. The left panels show the gating of cell population, the middle panels show DEAB-treated samples for setting the ALDH⁺ region and the right panels show the percentage of ALDH⁺ cells without DEAB. n=2. Tumorsphere formation assay for (C) SAS and (D) HSC3 cells transduced with shRNAs. n=3. Data were analyzed using the one-way ANOVA with a post-hoc Tukey's Honestly Significant Difference test. Scale bar, 100 μm. (E) Experimental flowchart of the *in vivo* tumor formation assay. Tumorsphere-derived SAS cells were transduced with shLacZ or shTRIB3, then injected subcutaneously (1x10⁴ cells/mouse) into nude mice (n=4) with shLacZ transduced cells injected at the left dorsal site and sh-TRIB3 transduced cells injected at the right dorsal site of each mouse. (F) Representative images of tumor-bearing mice and corresponding harvested tumors at day 30 for shLacZ-transduced cells and shTRIB3-transduced cells. Each row represents results from a single mouse. A ruler is included in tumor images for size reference. Data of tumor weights were presented as mean ± SEM and were analyzed using a unpaired Student's t-test. *P<0.05; ***P<0.001. TRIB3, tribbles pseudokinase 3; sh, short hairpin RNA; ALDH, aldehyde dehydrogenase; DEAB, diethylaminobenzaldehyde.

in SOX2 protein expression levels was observed in SAS cells following TRIB3 knockdown, which underscored the role of TRIB3 in the regulation of SOX2. Additionally, after knocking down TRIB3 in SAS cells, a significant decrease in the expression level of the E2F1 protein was observed (Fig. 4B). Upon overexpressing TRIB3 in OECM1 cells, the OSCC cell line with the lowest expression level of TRIB3 compared with SAS or HSC3 cells, a significant increase in the expression levels of both SOX2 and E2F1 was observed (Fig. 4C). The functional significance of SOX2 was examined via knockdown experiments, where silencing SOX2 led to a marked reduction in tumorsphere formation (Fig. 4D), confirming the critical role of SOX2 in terms of maintaining the stemness properties of OSCC cells.

As TRIB3 is a scaffold protein, which has been previously reported to enter the cell nucleus (16), it was hypothesized that TRIB3 may interact with E2F1, thereby leading to SOX2 transcription. First, it was demonstrated that the knockdown of TRIB3 in SAS cells led to a reduction in the SOX2 mRNA level (Fig. S6). Using the Eukaryotic Promoter Database to predict the potential E2F1 binding sites within the SOX2

promoter, two sites were identified [Fig. 4E; site 1 was located-551 bp from the transcriptional start site (TSS), whereas site 2 was located-16 bp from TSS]. ChIP assay was subsequently employed to show that, when TRIB3 expression was inhibited by transfection with a specific shRNA, the binding of E2F1 to the SOX2 promoter region at both binding sites was significantly reduced (Fig. 4F). Using a TRIB3 antibody to perform ChIP analysis, DNA fragments of the two E2F1 binding regions were also detected within the SOX2 promoter (Fig. 4G). Upon inhibiting E2F1 activity by treating the HSC3 cells with HLM006474, a pan-E2F inhibitor, a decrease in SOX2 protein expression was observed (Fig. 4H). Furthermore, the inhibition of E2F1 activity induced by HLM006474 in HSC3 cells also caused a decrease in tumorsphere formation (Fig. 4I).

It has previously been reported that SOX2 expression serves an important role in the self-renewal and tumorigenicity of OSCC CSCs (32). Using the GEPIA2 web server to analyze the HNC dataset of TCGA database, a significant positive correlation was found between SOX2 and TRIB3 at the mRNA level (Fig. S7A). It has been previously reported that E2F1 positively regulates SOX2 expression in HNC
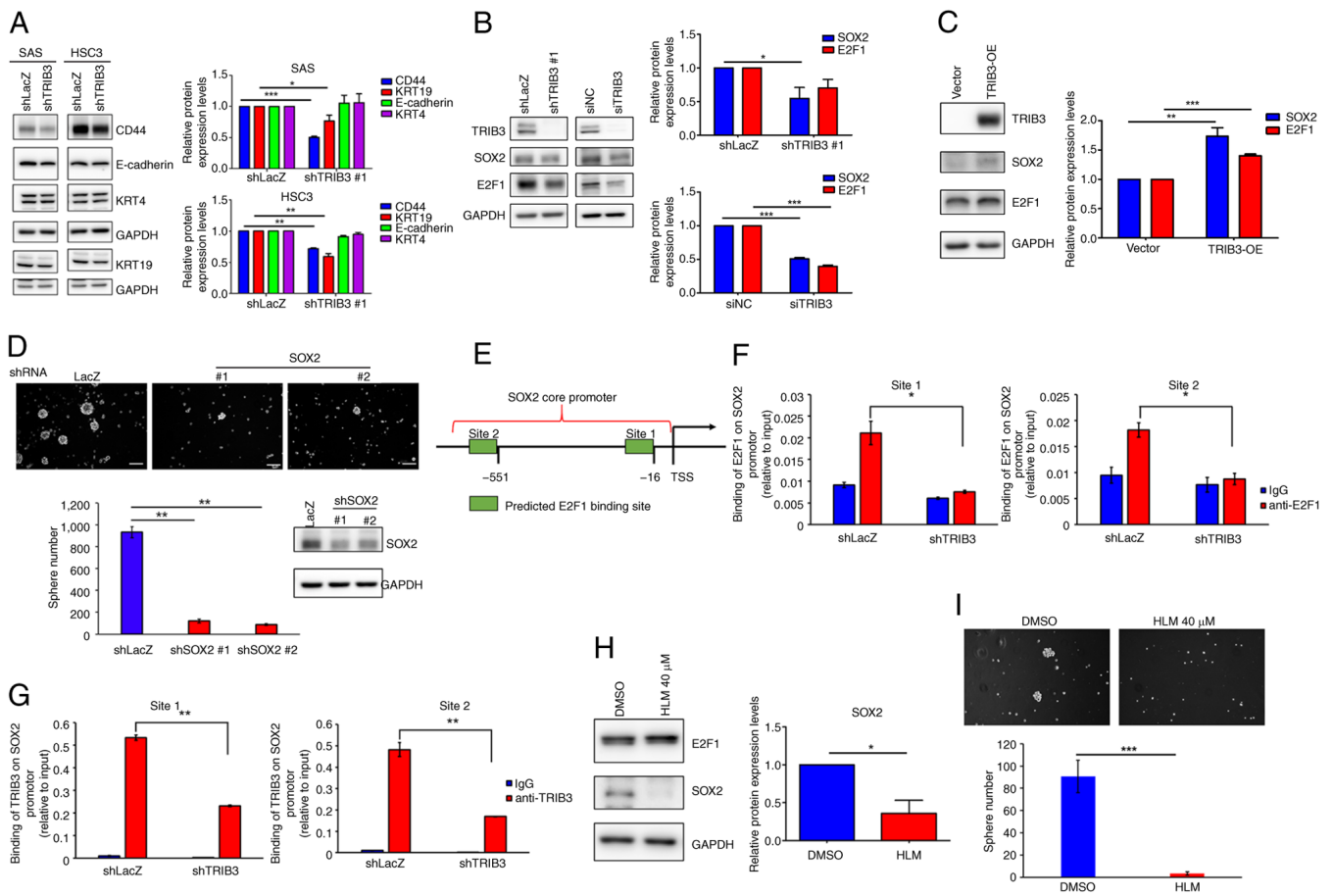
Figure 4. TRIB3 interacts with E2F1 in the nucleus to regulate SOX2 promoter activity in oral squamous cell carcinoma cells. (A) Western blotting analysis of CD44, E-cadherin, KRT4 and KRT19 protein expression levels in SAS and HSC3 cells transduced with shLacZ or shTRIB3. CD44, E-cadherin and KRT4 levels were normalized to the upper GAPDH band, while KRT19 levels were normalized to the lower GAPDH band. Blot images were representative of one of three independent experiments. (B) Western blotting analysis of TRIB3, SOX2 and E2F1 protein expression levels in SAS cells transfected with shLacZ, shTRIB3, siNC or siTRIB3 normalized to GAPDH. The protein expression levels of SOX2 and E2F1 in TRIB3 knockdown cells were compared with siNC or shLacZ cells. (C) Western blotting analysis of TRIB3, SOX2 and E2F1 protein expression levels in OEMC1 cells transfected with TRIB3-OE or an empty vector control normalized to GAPDH. (D) Tumorsphere formation assay of SAS cells transduced with shLacZ, sh-SOX2#1 or shSOX2#2 and the knockdown efficiency of shSOX2. (E) Schematic representation of predicted E2F1 binding sites within the SOX2 promoter. Chromatin immunoprecipitation followed by quantitative PCR analysis of (F) E2F1 and (G) TRIB3 binding to predicted sites within the SOX2 promoter in SAS cells transduced with shLacZ or shTRIB3#1. Effect of the E2F inhibitor HLM (40 μM) on HSC3 cells. (H) Western blotting analysis of SOX2 and E2F1 protein expression levels. (I) Tumorsphere formation assay. Scale bars, 100 μm. Data were presented as mean ± SD (n=3). The (A-C; F-H) Student's t-test or (D and I) one-way ANOVA with post-hoc Tukey's Honestly Significant Difference test were used for statistical analysis. *$P<0.05$; **$P<0.01$; ***$P<0.001$. TRIB3, tribbles pseudokinase 3; E2F1, E2F transcription factor 1; KRT, keratin; sh, short hairpin RNA; si, small interfering RNA; NC, negative control; OE, overexpression; TSS, transcriptional start site; HLM, HLM006474.

cells (33). The present study also identified a positive correlation between TRIB3 and E2F1 (Fig. S7B), as well as between E2F1 and SOX2 (Fig. S7C) mRNA levels in the HNC dataset from the TCGA database. These correlations, determined at both the mRNA and protein level, coupled with the findings obtained from previous studies, together provide a strong rationale for focusing on E2F1 and SOX2 as key downstream targets of TRIB3 in OSCC. As TRIB3 is a scaffold protein that can enter the cell nucleus (16), it was hypothesized that TRIB3 may interact with E2F1, thereby leading to SOX2 transcription. First, it was demonstrated that the knockdown of TRIB3 in SAS cells led to a reduction in the SOX2 mRNA level (Fig. S6). This suggested that the TRIB3-E2F1 complex exists in the nucleus of SAS cells, and potentially positively regulates SOX2 expression. The I-TASSER platform was used to build the 3D structures of TRIB3 and E2F1. The predicted 3D structures were then uploaded to the ZDOCK server to analyze

potential interaction regions between the two proteins. The results indicated that the C-terminal region of E2F1 potentially interacts with TRIB3 (Fig. 5A). Through immunoprecipitation analysis, a direct interaction between TRIB3 and E2F1 was identified in the nuclear protein fraction of SAS cells (Fig. 5B). By contrast, this interaction was found to be weak in the cytoplasmic protein fraction (Fig. S8). Collectively, these results suggested that the TRIB3-E2F1 complex was predominantly formed in the nucleus of SAS cells, which is consistent with its potential role in transcriptional regulation. Subsequently, the E2F1 protein was divided into two segments: The N-terminal (1-251 a.a.) and the C-terminal (252-437 a.a.) segments, which were cloned into a His-tagged plasmid used for investigating their interaction with full-length TRIB3, which was cloned into a plasmid with a HA-tag. These plasmids were then transfected into 293T cells and immunoprecipitation assays were performed. These results showed that the C-terminal region of
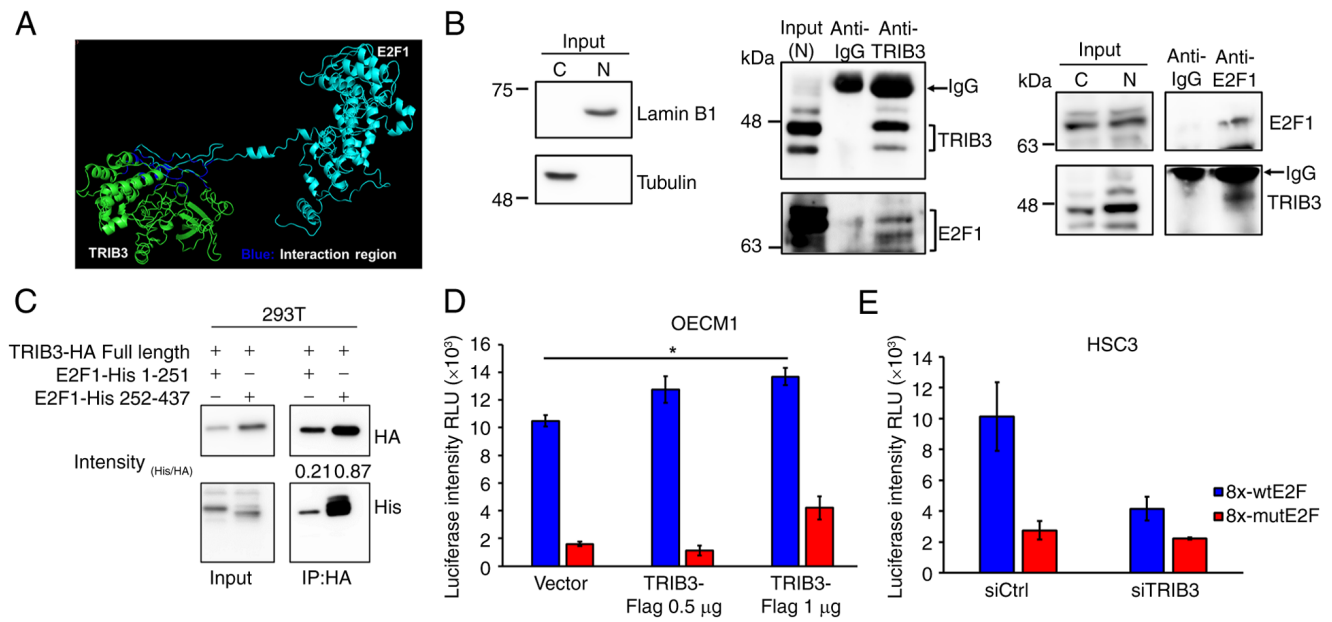
Figure 5. TRIB3 directly interacts with E2F1 and modulates its transcriptional activity. (A) Predicted protein-protein interaction between TRIB3 (green) and E2F1 (cyan). The 3D structure models generated by I-TASSER were input into the ZDOCK SERVER for interaction site prediction. The visualization was created using PyMol (version 2.4.1_198; Schrodinger) with manually annotated interacting amino acid residues shown in deep blue. (B) Western blotting analysis of C and N fractions from SAS tumorspheres, using Lamin B1 and Tubulin as N and C markers, respectively. Co-IP assays of N fractions using anti-TRIB3 or anti-E2F1 antibodies, with IgG as a negative control. (C) 293T cells co-transfected with HA-tagged full-length TRIB3 and His-tagged E2F1 fragments (1-251 or 252-437). (D) Luciferase reporter assay in OECM1 cells transfected with flag-tagged TRIB3 (0.5 or 1 µg) and luciferase vectors containing wildtype (8x-wtE2F) or mutant E2F1 DNA-binding sequences (8x-mutE2F). (E) Luciferase reporter assay in HSC3 cells transfected with luciferase vectors and siCtrl or siTRIB3. Data are presented as mean ± SD (n=3) and were analyzed one-way ANOVA with a post-hoc Tukey Honestly Significant Difference test or unpaired Student's t-test. *P<0.05. C, cytoplasmic; N nuclear; IP, immunoprecipitation; RLU, relative luminescence unit; ctrl, negative control; si, small interfering RNA; TRIB3, tribbles pseudokinase 3; E2F1, E2F transcription factor 1; HA, hemagglutinin; His, polyhistidine.

E2F1 predominantly interacted with TRIB3 (Fig. 5C). TRIB3 was subsequently overexpressed in OECM1 cells with 0.5 µg or 1.0 µg of TRIB3-flag plasmid, which resulted in a significantly increased level of E2F1 transcriptional activity in cells transfected with 1 µg of TRIB3-flag plasmid (Fig. 5D). Conversely, inhibition of TRIB3 expression in HSC3 cells led to a marked reduction in E2F1 transcriptional activity (Fig. 5E). To further identify the precise interaction sites between E2F1 and TRIB3, I-TASSER was used to analyze the TRIB3 protein structure and to predict the potential interaction sites with E2F1. These results demonstrated that the putative E2F1 interaction regions of TRIB3 were located at a.a. positions 107-110, 174-179, 236-240, 300-307 and 326-333 (Fig. S9A). To investigate these potential interactive regions, TRIB3 was segmented into three fragments: The N-terminal (1-180 a.a.), C-terminal (181-358 a.a.) and PKD (72-315 a.a.) regions (Fig. S9A). These fragments were built into an HA-tagged pcDNA vector, followed by co-transfection with a pCMV3 vector containing His-tagged E2F1 C-terminal sequences in 293T cells. The co-IP experiments demonstrated that TRIB3 fragments lacking regions a.a. 107-110 and a.a. 326-333 continued to interact with E2F1 (Fig. S9B). Therefore, it was hypothesized that the interaction sites between TRIB3 and E2F1 may have been located at a.a. 174-179 or a.a. 236-240. To further refine the nature of the interaction site, three HA-tagged TRIB3 mutants were generated: These included one with a deletion at a.a. 174-179, another with a deletion at a.a. 236-240 and a third with both regions deleted. Co-IP analysis using anti-HA antibodies for IP, followed by immunoblotting with anti-His antibodies,

showed that deletion of a.a. 236-240 led to a reduction in E2F1-His co-precipitation. By contrast, deletion of a.a. 174-179 had no such effect (Fig. S9C). These results suggested that the putative interaction site between TRIB3 and E2F1 was likely located at a.a. 236-240. Taken together, these results indicated that TRIB3 may directly interact with E2F1 to regulate its transcriptional activity, thereby increasing SOX2 expression and participating in the self-renewal of OSCC-CSCs.

TRIB3 maintains EGFR protein expression through preventing lysosomal degradation. A previous study reported that EGFR signaling promotes the formation of OSCC-CSCs (34). Knockdown of TRIB3 in SAS or HSC3 cells led to a decrease in the protein expression level of EGFR and the decreased activation of EGFR signaling, including the phosphorylation of EGFR and ERK1/2 (Fig. 6A). Conversely, overexpression of TRIB3 in OECM1 cells led to a significant increase in EGFR protein expression levels compared with the control group (Fig. 6B). Degradation of receptor tyrosine kinases by lysosomes has been shown to regulate their signaling strength (35). Additionally, TRIB3 expression in hepatic stellate cells may impede the process of lysosome-mediated late endosome degradation (36). Therefore, it was hypothesized that TRIB3 may regulate lysosomal activity in OSCC cells to maintain EGFR expression levels. The knockdown of TRIB3 in SAS cells significantly increased lysosomal activity (Fig. 6C). Chloroquine inhibits lysosome activity (37). The downregulation of EGFR caused by TRIB3 knockdown was significantly restored by chloroquine treatment at a concentration of 30 mM (Fig. 6D). Furthermore,
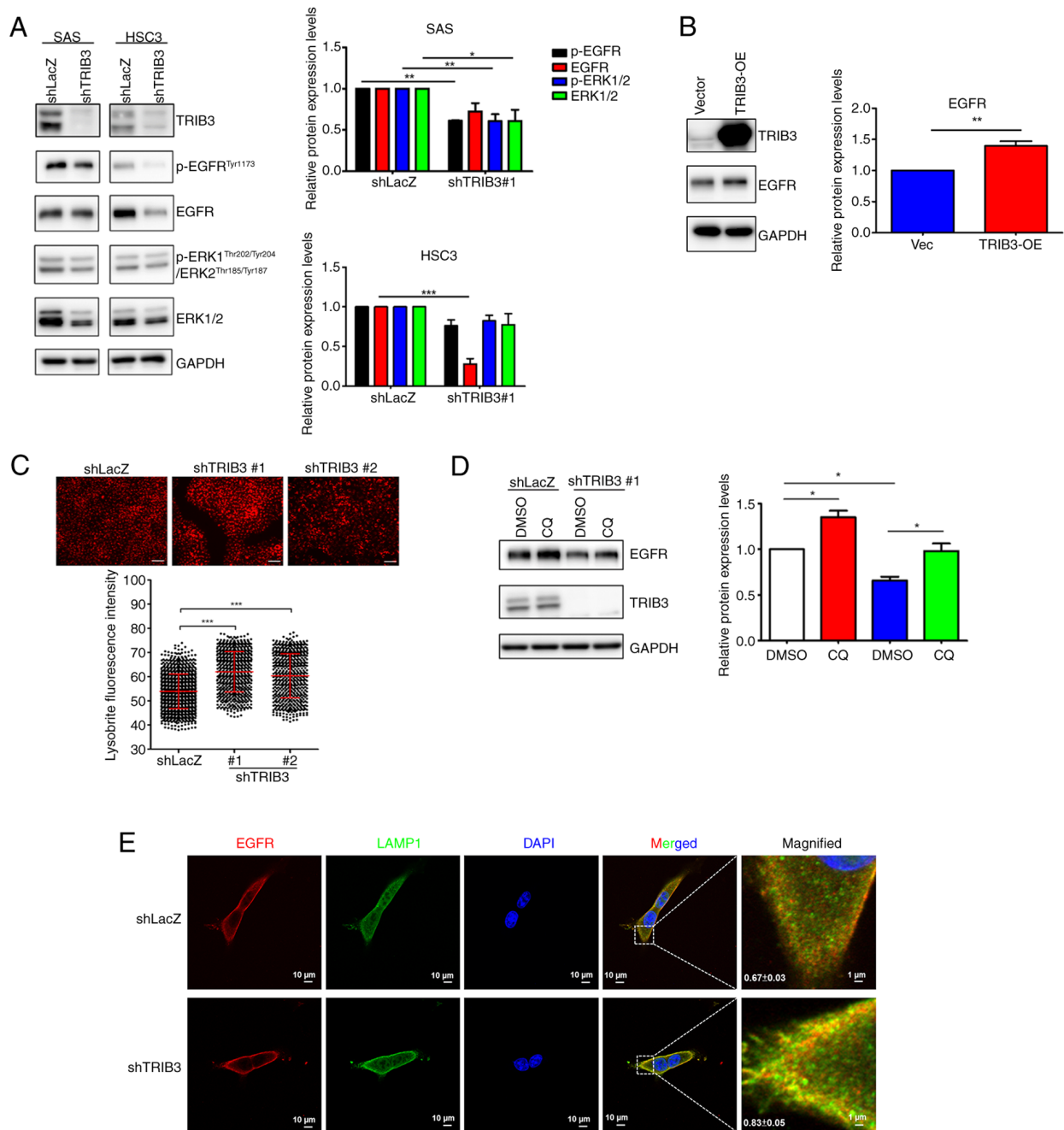
Figure 6. TRIB3 regulates EGFR expression by modulating lysosomal activity. (A) Western blotting analysis of TRIB3, total and p-EGFR^{Tyr1173} and total and p-ERK1$^{Thr202/Tyr204}$/ERK2$^{Thr185/Tyr187}$ in SAS and HSC3 cells transduced with shLacZ or shTRIB3#1 normalized to GAPDH. n=3. The quantitative values in the shTRIB3 group were compared with those in the shLacZ group. (B) Western blotting analysis of TRIB3 and EGFR in OECM1 cells transfected with TRIB3-OE or empty vector control normalized to GAPDH. n=3. (C) Lysosomal activity assay in SAS cells transduced with shLacZ, shTRIB3#1 or shTRIB3#2 stained with Lysotracker-Red. Representative fluorescence microscopy images and quantification of red fluorescence intensity in individual cells using ImageJ software (version 1.54k; National Institutes of Health). Scale bars, 100 μm. n=2. (D) Western blotting analysis of TRIB3 and EGFR in SAS cells transduced with shLacZ or shTRIB3#1 and treated with 30 μM CQ or 0.1% DMSO normalized to GAPDH. (E) Confocal microscopy images of SAS cells transduced with shLacZ or shTRIB3#1, immunostained for EGFR (red), LAMP1 (green) and with DAPI (blue). Pearson's correlation coefficients for EGFR-LAMP1 colocalization are shown in the lower-left corners of merged images. n=3. Scale bars, 10 μm or 1 μm. Data are presented as mean ± SD. Data were analyzed using the Student's t-test or the one-way ANOVA with a post-hoc Tukey's Honestly Significant Difference test. *P<0.05; **P<0.01; ***P<0.001. OE, overexpression; CQ, chloroquine; p, phosphorylated; TRIB3, tribbles pseudokinase 3; sh, short hairpin RNA; vec, empty vector.

immunofluorescence staining showed that when TRIB3 expression was suppressed in SAS cells, the colocalization of EGFR and lysosomal-associated membrane protein 1, a lysosomal marker protein, was significantly increased (Fig. 6E). Taken together, these results suggested that the expression of TRIB3 in OSCC cells regulated lysosomal activity, thereby contributing to the maintenance of EGFR expression.

Correlation of TRIB3 expression levels with key regulatory molecules in xenograft tumors and human OSCC specimens. Subsequently, the expression levels of cell cycle-associated factors CDK1, CDK6, E2F1, SOX2 and EGFR were measured, which are key molecules implicated in TRIB3-regulated cell proliferation and CSC activity. Immunohistochemical staining of xenograft tumor tissues demonstrated a significant reduction
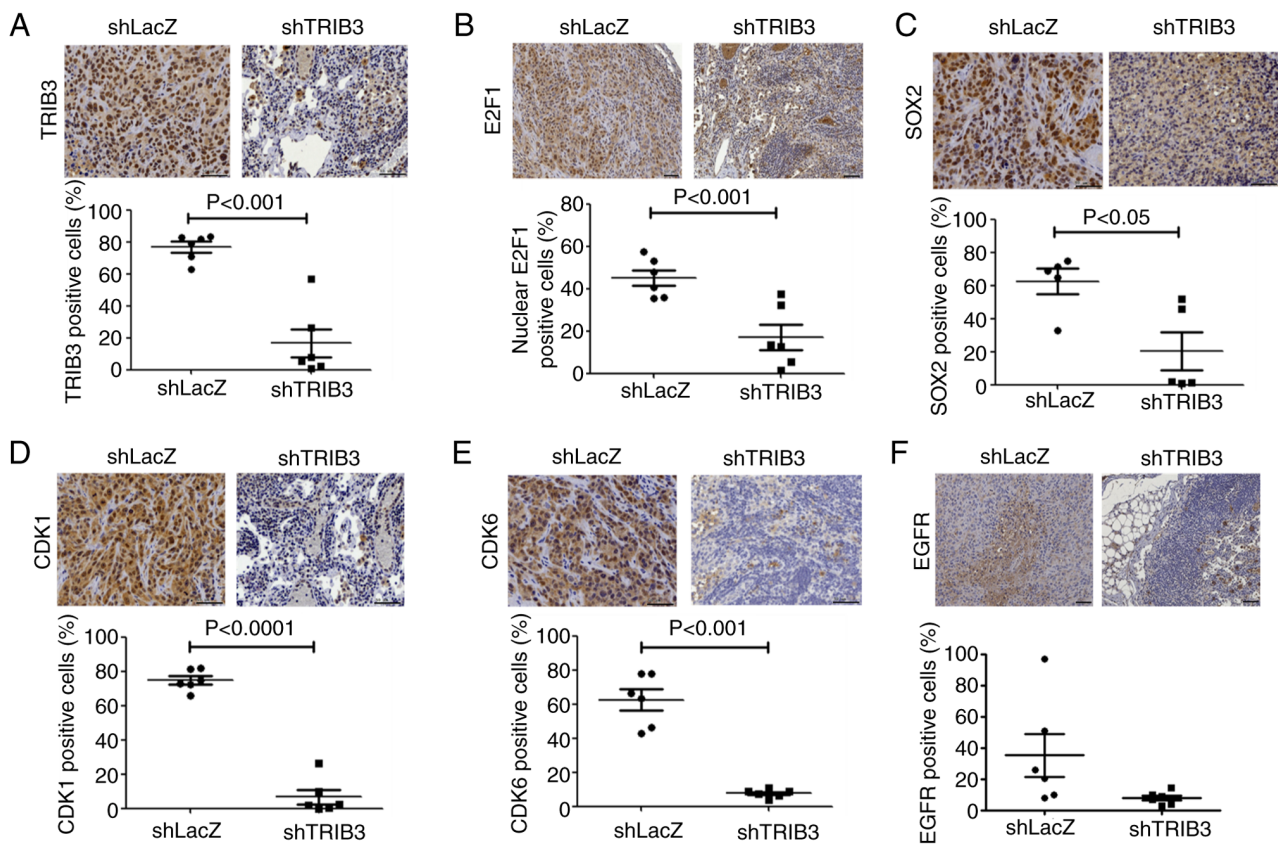
Figure 7. Knockdown of TRIB3 downregulates cell cycle and stemness markers in xenograft tumors. Tumors derived from SAS cells transduced with shLacZ or shTRIB3 were analyzed by immunohistochemistry. Sections were stained for (A) TRIB3, (B) E2F1, (C) SOX2, (D) CDK1, (E) CDK6 and (F) EGFR. Representative immunohistochemical images are presented for each protein. Quantification of positive cells for each marker are presented. Staining intensities were quantitatively assessed from two random objective fields across three independent tumor sections per group. Data are presented as mean ± SD. Statistical analysis was performed using the unpaired Student's t-test. Scale bar, 50 μm. TRIB3, tribbles pseudokinase 3; E2F1, E2F transcription factor 1; sh, short hairpin RNA.

in TRIB3 (Fig. 7A), E2F1 (Fig. 7B), SOX2 (Fig. 7C), CDK1 (Fig. 7D) and CDK6 (Fig. 7E) expression levels in the shTRIB3 group compared with the controls. A marked decrease in EGFR expression levels following TRIB3 knockdown was observed (Fig. 7F). This suggested a potential regulatory association between TRIB3 and EGFR *in vivo*. Furthermore, these associations were analyzed in human HNC tissue array slides, which included 70 HNC cases. Representative images of high and low expression levels of TRIB3, E2F1, SOX2 and EGFR were produced (Fig. 8A). Significant positive correlations were observed between TRIB3 and E2F1 (Fig. 8B), TRIB3 and SOX2 (Fig. 8C), E2F1 and SOX2 (Fig. 8D) and TRIB3 and EGFR (Fig. 8E). In the HNSC RNA-seq dataset from the TCGA database, the Hallmark_E2F_Targets gene set were enriched in samples with high TRIB3 expression levels when using the median as a cut-off value (Fig. S10A). In addition, the EGFR-associated gene set was enriched in samples with high median TRIB3 mRNA expression levels (Fig. S10B). Collectively, these results suggested that the expression of TRIB3 may maintain OSCC-CSC tumorigenicity through the regulation of E2F1/SOX2 or EGFR expression.

Discussion

To the best of our knowledge, the present study is the first to report the mechanistic link between TRIB3, E2F1 and SOX2

in the context of OSCC stemness. Additionally, the present study explored the role of TRIB3 in regulating EGFR stability via lysosomal degradation in OSCC cells. Although it was demonstrated that TRIB3 was a poor prognostic factor in the HNC dataset from the TCGA database, future studies incorporating more detailed clinicopathological data and larger patient cohorts could further the understanding of the role of TRIB3 in OSCC progression and patient outcomes. The results of the present study, including a reduced rate of colony formation and decreased BrdU incorporation, suggested a cell cycle arrest of OSCC cells following TRIB3 knockdown, as evidenced by the decreased expression levels of CDK6 in both SAS and HSC3 cells. As different cell lines were used in these experiments, it was expected that there would be some variability in the results obtained between cell lines. The CDK4/6 inhibitor experiments demonstrated that when CDK4/6 activity was inhibited, there was a concentration-dependent reduction in the proliferation of both OSCC cell lines, which could potentially be explained by the findings of the western blotting analysis, whereby a significant decrease in CDK6 expression levels was observed in both OSCC cell lines after TRIB3 knockdown. This suggested that TRIB3 may not affect all cell cycle-related proteins simultaneously, but rather regulated the proliferation of OSCC cells through its role in CDK6 expression.

Although the present study focused on cell cycle dynamics, it is possible that TRIB3 knockdown may also influence
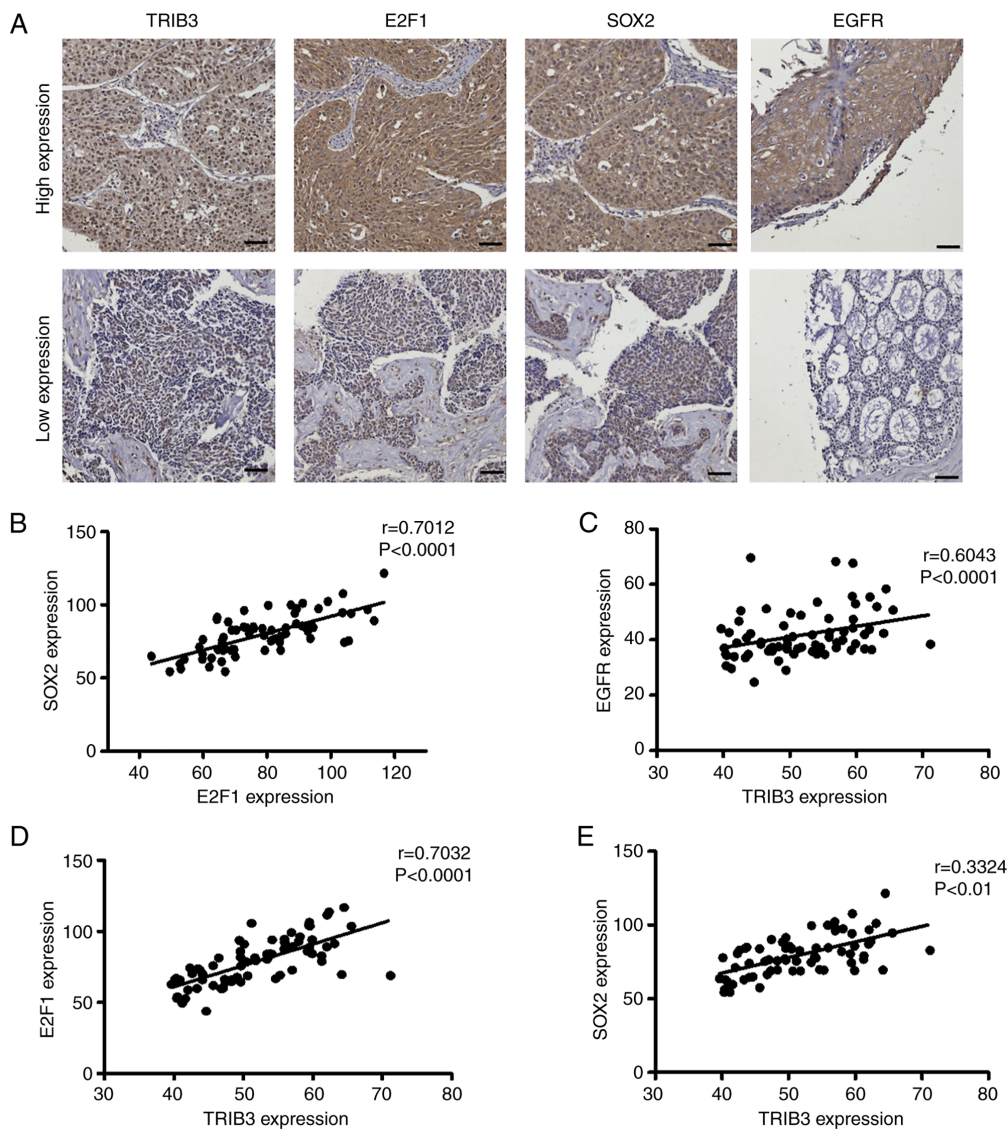
Figure 8. TRIB3 expression is positively correlated with E2F1, SOX2 and EGFR expression in HNC tissues. (A) Representative immunohistochemistry images of TRIB3, E2F1, SOX2 and EGFR expression in human HNC tissue microarray samples. Scale bar, 50 μm. Correlation analyses of protein expression levels in 70 HNC tissue samples: (B) TRIB3 vs. E2F1 (C) TRIB3 vs. SOX2 (D) E2F1 vs. SOX2 and (E) TRIB3 vs. EGFR. Staining intensities were quantified using TissueFAXS software (version 7.0; TissueGnostics GmbH) and expressed as pixel density. Correlations were analyzed using Pearson's correlation coefficient (r). n=70. TRIB3, tribbles pseudokinase 3; IHC, immunohistochemistry; E2F1, E2F transcription factor 1; HNC, head and neck cancer.

other cellular processes, including senescence, apoptosis and differentiation. In the present study, TRIB3 knockdown did not induce apoptosis, as evidenced by the unchanged levels of cleaved caspase-3 in the SAS and HSC3 OSCC cells. However, it was noted that TRIB3 silencing could induce cellular senescence, as evidenced by the presence of increased senescence-associated heterochromatin foci with DAPI puncta and an increase in H2AX phosphorylation at residue Ser-139. Cellular senescence has been suggested as an internal mechanism to prevent tumorigenesis, although persistent senescence in tumor cells can lead to treatment resistance (38). A combination of MEK and CDK4/6 inhibitors has been reported to induce cell senescence to suppress the proliferation of pancreatic ductal adenocarcinoma (PDAC) cells and to trigger angiogenesis according to the senescence-associated secretory phenotype (SASP) to enhance the delivery of chemotherapeutic agents in PDAC xenograft tumors (39). Further investigation is warranted to elucidate the role of TRIB3 with

respect to the regulation of cellular senescence and the SASP phenotype in OSCC cells. Shen et al (17) previously reported that knockdown of TRIB3 in SCC9 OSCC cells decreased in vivo tumorigenic properties and that this was associated with the upregulation of Akt/mTOR activation. In the present study, it was demonstrated that TRIB3 functioned as an oncogenic protein in OSCC cells and potentially served a role in the maintenance of OSCC-CSCs.

The present study also demonstrated that TRIB3 bound to E2F1 and that this process was involved in SOX2 expression in OSCC cells. Furthermore, knocking down TRIB3 protein expression also downregulated E2F1 expression, whereas overexpression of TRIB3 led to an increase in the protein expression level of E2F1. The reduced precipitation of E2F1-bound SOX2 promoter fragments in TRIB3-knockdown cells observed in the ChIP experiments may have resulted from either reduced TRIB3-E2F1 interaction or the downregulation of E2F1 protein expression in these cells. The regulatory role of

TRIB3 in E2F1 transcriptional activity requires further investigation. Although the results of the present study supported the hypothesis that there existed an interaction with TRIB3 involving the C-terminus of E2F1 and the putative interaction site between TRIB3 and E2F1 was likely located at a.a. 236-240. This implied that TRIB3 may bind to the C-terminal transactivation domain of E2F1 through the C-terminal region of its PKD domain. However, the possibility that the region spanning a.a. 300-307 may be another site of interaction with E2F1 could not be excluded. Further investigation using deletion mutants with single mutations at a.a. 300-307, as well as double mutations at a.a. 236-240 and 300-307, are needed to confirm this hypothesis. Taken together, these results suggested that the putative interaction site of TRIB3 with E2F1 was likely to be located at a.a. 174-179. This implied that TRIB3 may bind to the C-terminal transactivation domain of E2F1 through its N-terminal of the PKD domain. However, it is important to note that the precise sites within E2F1 require further investigation, using site-specific mutants or additional deletion mutants. The Hallmark_E2F_Targets gene set was markedly enriched in samples with high TRIB3 expression levels in the HNSC RNA-seq dataset from the TCGA database This enrichment of E2F target genes was particularly significant as E2F transcription factors are key regulators of cell cycle progression and cell proliferation. E2F targets include genes essential for G1/S transition and DNA replication (40), suggesting that high TRIB3 expression may promote cell cycle progression through an E2F-dependent mechanism. This finding is consistent with our observed phenotypes of reduced cell proliferation upon TRIB3 knockdown and provides a potential mechanistic link between TRIB3 expression and cell cycle regulation in OSCC cells. Furthermore, this association between TRIB3 and E2F target genes may partially explain the oncogenic function of TRIB3 that contributes to OSCC progression.

The findings of the present study on the role of TRIB3 in OSCC-CSC formation have added to the growing body of evidence on the complex regulation of E2F1 and its downstream targets. A previous study showed that EGFR/RAS signaling is able to post-transcriptionally upregulate the expression level of E2F1 in *Drosophila* midgut enterocytes (41). Additionally, it has been shown that suppression of proteasome 26S subunit, non-ATPase 14, a deubiquitinating enzyme, leads to reduced protein expression levels of both E2F1 and SOX2 in SCC15 and UM1 OSCC cells (33). These findings suggest that multiple layers of regulation exist for the control of E2F1 activity. Although the role of TRIB3 in EGFR recycling has been previously demonstrated in lung cancer cells (42), the present study has extended this knowledge to encompass OSCC-CSCs, suggesting a potentially conserved mechanism across different cancer types. However, the specific role of reduced EGFR signaling in the downregulation of E2F1 in TRIB3-knockdown OSCC cells requires further investigation. Moreover, the potential role of TRIB3 in regulating E2F1 activity through post-transcriptional modifications, including ubiquitination and deubiquitination processes, presents an avenue for future studies. These studies could potentially provide us with a more comprehensive understanding of the TRIB3-E2F1-SOX2 axis in OSCC-CSC formation and maintenance.

Yu *et al* (43) reported that TRIB3 prevented the ubiquitination-mediated degradation of FOXO1, which led to an increased level of SOX2 transcription, thereby enhancing the self-renewal capability of breast CSCs. The involvement of TRIB3 in preventing the ubiquitination of SOX2 or EGFR, which would increase their stability in OSCC cells, is a hypothesis that could be investigated by cycloheximide chase experiments in future studies. In breast cancer, a peptide designed to mimic a.a. residues 191-204 of the Akt protein was found to bind to TRIB3 (43). Treatment of breast cancer cells with this peptide reduced their ability to form tumorspheres, suggesting that inhibiting TRIB3-Akt interactions could suppress breast CSCs (43). In the future, peptide drugs could be designed to disrupt the interaction between TRIB3 and E2F1 in order to test whether they can inhibit both the transcriptional activity of E2F1 and the impact on OSCC-CSC self-renewal. It was demonstrated in the present study that E2F1-His bound to all three TRIB3 mutants: Del 174-179, del 236-240 and the double deletions. However, a reduction in binding was specifically detected in the del 236-240 mutant, suggesting this region may be a key interaction site. Despite this, the presence of some binding with all mutants, including the double deletion, indicated that the precise role of other regions, such as a.a. 300-307, requires further investigation. Therefore, the current data present a limitation in fully defining the binding sites between TRIB3 and E2F1. This uncertainty may impact the design of peptide-based drugs targeting these interactions, as the exact binding regions remain to be conclusively identified. Further studies, including the analysis of additional mutants, are necessary to refine the understanding of the interaction sites. Other challenges associated with peptide drugs also need to be considered, including their susceptibility to degradation by proteases following administration (44) and the potential risk of immunogenicity from synthetic peptides (45).

The results of the present study demonstrated that TRIB3 was able to regulate lysosomal activity to maintain the expression of EGFR. Transcription factor EB (TFEB) is a master regulator in the biogenesis of lysosomes (46). Ferron *et al* (47) reported that TFEB can be phosphorylated by protein kinase C (PKC), thereby maintaining its stability and promoting lysosome biogenesis. Yu *et al* (42) reported that knockdown of TRIB3 resulted in a reduction in the expression level of PKC protein. TRIB3 may regulate lysosome biogenesis through the PKC-mediated phosphorylation of TFEB. In the HNC RNA-seq dataset derived from TCGA database, it was shown that the EGFR-associated gene set was markedlyenriched in samples with high median expression levels of TRIB3 mRNA. However, the finding that TRIB3 may positively regulate EGFR expression in OSCC cell lines was further verified on the basis of the IHC data from the HNC tissue microarray. Yin *et al* (48) reported that LY2835219, a CDK4/6 inhibitor, induced lysosomal biogenesis in multiple cell lines, including HepG2 liver cancer cells. In the present study, the decreased expression of the CDK6 protein in SAS and HSC3 cells was observed following knockdown of TRIB3. Moreover, an increased fluorescence intensity of the lysotracker may potentially be induced by the suppression of CDK6 expression, although this aspect requires further investigation.

Lv *et al* (49) reported that inhibition of EGFR activation in HNC cells using the tyrosine kinase inhibitor (TKI) gefitinib

led to decreased expression levels of SOX2. SOX2 interacts directly with EGFR, preventing SOX2 degradation via autophagy. In lung cancer cells, resistance to TKIs targeting EGFR could increase SOX2 expression levels (50). In addition, it was reported that there is a positive feedback loop between SOX2 and EGFR in lung cancer/progenitor cells (51). However, SOX2 expression is detectable in adult stem or progenitor cells and this may serve a role in the maintenance of adult tissue, such as promoting the differentiation of neural stem cells into neuronal or glial cells (52). Therefore, therapies involving small molecule inhibitors of SOX2 may be associated with considerable side effects (53). Several small molecule compounds have been reported to inhibit SOX2 expression, such as the lysine-specific demethylase 1 inhibitor CBB1007, which was found to decrease SOX2 expression via increasing the binding of lysine-9-methylated histone 3 to the SOX2 gene locus (54). In OSCC, it may be possible to develop a combination therapy of EGFR-TKIs with non-specific inhibitors to decrease the expression level of SOX2, thereby reducing the development of EGFR-TKI resistance and successfully decreasing the population of CSCs.

Although the present study demonstrated the oncogenic role of TRIB3 in OSCC cells through regulating SOX2 expression via recruitment of E2F1 to the SOX2 promoter, and maintaining EGFR expression occurs via preventing lysosomal degradation, certain limitations should be acknowledged. For example, it remains to be investigated whether disrupting the interaction between E2F1 and TRIB3 exerts any suppressive effect on OSCC cells. Moreover, the mechanism through which TRIB3 regulates lysosomal activity in OSCC cells requires future exploration. Finally, to evaluate the therapeutic potential of these findings in OSCCs, the ensuing development of TRIB3 inhibitors that either suppress its expression or inhibit its protein scaffolding activity is necessary.

In conclusion, the present study provided evidence suggesting that TRIB3 may serve a critical role in OSCC development. An elevated expression level of TRIB3 was found to be correlated with poor patient prognosis, and this was implicated in driving cell proliferation and self-renewal in OSCC and OSCC-CSCs. Mechanistically, TRIB3 interacted with E2F1 to augment SOX2 expression, thereby fostering self-renewal capabilities. Moreover, TRIB3 stabilized the EGFR protein through inhibiting its lysosomal degradation, a process that contributed to signaling cascades relevant to CSCs. Taken together, the findings of the present study demonstrated a dual role of TRIB3 in OSCC: It contributed to the regulation of cell proliferation and supported the maintenance of CSC characteristics within OSCC. These findings not only suggest that TRIB3 has a potential role as an oncogene, but also highlighted its value as a therapeutic target for the future management of OSCC.

Acknowledgements

Funding

Availability of data and materials

The data generated in the present study may be requested from the corresponding author.

Authors' contributions

Y-MH, Y-HH, L-SH and W-WC were responsible for conceptualization of the study. Y-MH, Y-HH, P-JC and W-LW were responsible for data curation. Y-HH, P-JC, W-LW and W-WC were responsible for data analysis. Y-MH and W-WC obtained the funding. Y-MH. Y-HH and W-WC wrote the manuscript and L-SH and W-WC reviewed and edited the manuscript. All authors read and approved the final version of the manuscript. Y-HH, Y-MH and W-WC confirm the authenticity of all the raw data.

Ethics approval and consent to participate

The use of the HNC tissue microarray for the present study was approved by the Chang Gung Medical Foundation Institutional Review Board (approval no. 202002207B0C501; Taoyuan, Taiwan). The animal experiments were approved by the Institutional Animal Care and Use Committee at Chung Shan Medical University (approval no. 2437; Taichung, Taiwan).

Patient consent for publication

Not applicable.

Competing interests

The authors declare that they have no competing interests.

Use of artificial intelligence tools

ChatGPT (version 4.0) and Claude 3.5 Sonnet were used to improve the readability and language of the manuscript. All revisions made by the artificial intelligence tools were reviewed for accuracy and consistency to ensure the original meaning of the text was maintained.

References

1. Bugshan A and Farooq I: Oral squamous cell carcinoma: Metastasis, potentially associated malignant disorders, etiology and recent advancements in diagnosis. F1000Res 9: 229, 2020.
2. Antra, Parashar P, Hungyo H, Jain A, Ahmad S and Tandon V: Unraveling molecular mechanisms of head and neck cancer. Crit Rev Oncol Hematol 178: 103778, 2022.
3. Hsiao JR, Chang CC, Lee WT, Huang CC, Ou CY, Tsai ST, Chen KC, Huang JS, Wong TY, Lai YH, et al: The interplay between oral microbiome, lifestyle factors and genetic polymorphisms in the risk of oral squamous cell carcinoma. Carcinogenesis 39: 778-787, 2018.

4. Almangush A, Leivo I and Mäkitie AA: Biomarkers for immunotherapy of oral squamous cell carcinoma: Current status and challenges. Front Oncol 11: 616629, 2021.
5. Patil S, Al-Brakati A, Abidi NH, Almasri MA, Almeslet AS, Patil VR, Raj AT and Bhandi S: CD44-positive cancer stem cells from oral squamous cell carcinoma exhibit reduced proliferation and stemness gene expression upon adipogenic induction. Med Oncol 39: 23, 2022.
6. Swain N, Thakur M, Pathak J, Patel S and Hosalkar R: Aldehyde dehydrogenase 1: Its key role in cell physiology and oral carcinogenesis. Dent Med Probl 59: 629-635, 2022.
7. Fukumoto C, Uchida D and Kawamata H: Diversity of the origin of cancer stem cells in oral squamous cell carcinoma and its clinical implications. Cancers (Basel) 14: 3588, 2022.
8. Yang L, Shi P, Zhao G, Xu J, Peng W, Zhang J, Zhang G, Wang X, Dong Z, Chen F and Cui H: Targeting cancer stem cell pathways for cancer therapy. Signal Transduct Target Ther 5: 8, 2020.
9. Stefanovska B, André F and Fromigué O: Tribbles pseudokinase 3 regulation and contribution to cancer. Cancers (Basel) 13: 1822, 2021.
10. Salazar M, Lorente M, Garcia-Taboada E, Pérez Gómez E, Dávila D, Zúñiga-García P, María Flores J, Rodríguez A, Hegedus Z, Mosén-Ansorena D, *et al*: Loss of tribbles pseudokinase-3 promotes Akt-driven tumorigenesis via FOXO inactivation. Cell Death Differ 22: 131-144, 2015.
11. Yu Y, Qiu L, Guo J, Yang D, Qu L, Yu J, Zhan F, Xue M and Zhong M: TRIB3 mediates the expression of Wnt5a and activation of nuclear factor-κB in porphyromonas endodontalis lipopolysaccharide-treated osteoblasts. Mol Oral Microbiol 30: 295-306, 2015.
12. Cao X, Fang X, Guo M, Li X, He Y, Xie M, Xu Y and Liu X: TRB3 mediates vascular remodeling by activating the MAPK signaling pathway in hypoxic pulmonary hypertension. Respir Res 22: 312, 2021.
13. Vidal L, Victoria I, Gaba L, Martín MG, Brunet M, Colom H, Cortal M, Gómez-Ferrería M, Yeste-Velasco M, Perez A, *et al*: A first-in-human phase I/Ib dose-escalation clinical trial of the autophagy inducer ABTL0812 in patients with advanced solid tumours. Eur J Cancer 146: 87-94, 2021.
14. Erazo T, Lorente M, López-Plana A, Muñoz-Guardiola P, Fernández-Nogueira P, García-Martínez JA, Bragado P, Fuster G, Salazar M, Espadaler J, *et al*: The new antitumor drug ABTL0812 inhibits the Akt/mTORC1 axis by upregulating tribbles-3 pseudokinase. Clin Cancer Res 22: 2508-2519, 2016.
15. Qu J, Liu B, Li B, Du G, Li Y, Wang J, He L and Wan X: TRIB3 suppresses proliferation and invasion and promotes apoptosis of endometrial cancer cells by regulating the AKT signaling pathway. Onco Targets Ther 12: 2235-2245, 2019.
16. Wang WL, Hong GC, Chien PJ, Huang YH, Lee HT, Wang PH, Lee YC and Chang WW: Tribbles pseudokinase 3 contributes to cancer stemness of endometrial cancer cells by regulating β-catenin expression. Cancers (Basel) 12: 3785, 2020.
17. Shen P, Zhang TY and Wang SY: TRIB3 promotes oral squamous cell carcinoma cell proliferation by activating the AKT signaling pathway. Exp Ther Med 21: 313, 2021.
18. Lacazette E: A laboratory practical illustrating the use of the ChIP-qPCR method in a robust model: Estrogen receptor alpha immunoprecipitation using Mcf-7 culture cells. Biochem Mol Biol Educ 45: 152-160, 2017.
19. Iglesias-Ara A, Osinalde N and Zubiaga AM: Detection of E2F-induced transcriptional activity using a dual luciferase reporter assay. In: The Retinoblastoma Protein. Santiago-Cardona PG (ed). Springer New York, New York, NY, pp153-166, 2018.
20. Yang J and Zhang Y: I-TASSER server: New development for protein structure and function predictions. Nucleic Acids Res 43 (W1): W174-W181, 2015.
21. Song W, Zhang WH, Zhang H, Li Y, Zhang Y, Yin W and Yang Q: Validation of housekeeping genes for the normalization of RT-qPCR expression studies in oral squamous cell carcinoma cell line treated by 5 kinds of chemotherapy drugs. Cell Mol Biol (Noisy-le-grand) 62: 29-34, 2016.
22. Livak KJ and Schmittgen TD: Analysis of relative gene expression data using real-time quantitative PCR and the 2(-Delta Delta C(T)) method. Methods 25: 402-408, 2001.
23. Finn RS, Martin M, Rugo HS, Jones S, Im SA, Gelmon K, Harbeck N, Lipatov ON, Walshe JM, Moulder S, *et al*: Palbociclib and letrozole in advanced breast cancer. N Engl J Med 375: 1925-1936, 2016.
24. Burcham ZM, Pechal JL, Schmidt CJ, Bose JL, Rosch JW, Benbow ME and Jordan HR: Bacterial community succession, transmigration, and differential gene transcription in a controlled vertebrate decomposition model. Front Microbiol 10: 745, 2019.
25. Marx JO, Brice AK, Boston RC and Smith AL: Incidence rates of spontaneous disease in laboratory mice used at a large biomedical research institution. J Am Assoc Lab Anim Sci 52: 782-791, 2013.
26. Patil S: CD44 sorted cells have an augmented potential for proliferation, epithelial-mesenchymal transition, stemness, and a predominantly inflammatory cytokine and angiogenic secretome. Curr Issues Mol Biol 43: 423-433, 2021.
27. Ghuwalewala S, Ghatak D, Das P, Dey S, Sarkar S, Alam N, Panda CK and Roychoudhury S: CD44(high)CD24(low) molecular signature determines the cancer stem cell and EMT phenotype in oral squamous cell carcinoma. Stem Cell Res 16: 405-417, 2016.
28. Abbas O, Richards JE, Yaar R and Mahalingam M: Stem cell markers (cytokeratin 15, cytokeratin 19 and p63) in in situ and invasive cutaneous epithelial lesions. Mod Pathol 24: 90-97, 2011.
29. Menz A, Bauer R, Kluth M, Marie von Bargen C, Gorbokon N, Viehweger F, Lennartz M, Völkl C, Fraune C, Uhlig R, *et al*: Diagnostic and prognostic impact of cytokeratin 19 expression analysis in human tumors: A tissue microarray study of 13,172 tumors. Hum Pathol 115: 19-36, 2021.
30. Nascimento RB, Machado IAR, Silva JC, Faria LAS, Borba FC, Porto LPA, Santos JN, Ramalho LMP, Rodini CO, Rodrigues MFSD, *et al*: Differential expression of cadherins switch and caveolin-2 during stages of oral carcinogenesis. J Oral Maxillofac Pathol 27: 507-514, 2023.
31. Sakamoto K, Aragaki T, Morita K, Kawachi H, Kayamori K, Nakanishi S, Omura K, Miki Y, Okada N, Katsube K, *et al*: Down-regulation of keratin 4 and keratin 13 expression in oral squamous cell carcinoma and epithelial dysplasia: A clue for histopathogenesis. Histopathology 58: 531-542, 2011.
32. Lee SH, Oh SY, Do SI, Lee HJ, Kang HJ, Rho YS, Bae WJ and Lim YC: SOX2 regulates self-renewal and tumorigenicity of stem-like cells of head and neck squamous cell carcinoma. Br J Cancer 111: 2122-2130, 2014.
33. Jing Y, Duan Y, Zhou M, Yue K, Zhuo S, Li X, Liu D, Ye B, Lai Q, Li L, *et al*: Blockade of deubiquitinating enzyme PSMD14 overcomes chemoresistance in head and neck squamous cell carcinoma by antagonizing E2F1/Akt/SOX2-mediated stemness. Theranostics 11: 2655-2669, 2021.
34. Xu Q, Zhang Q, Ishida Y, Hajjar S, Tang X, Shi H, Dang CV and Le AD: EGF induces epithelial-mesenchymal transition and cancer stem-like cell properties in human oral cancer cells via promoting Warburg effect. Oncotarget 8: 9557-9571, 2017.
35. Miaczynska M: Effects of membrane trafficking on signaling by receptor tyrosine kinases. Cold Spring Harb Perspect Biol 5: a009035, 2013.
36. Zhang XW, Zhou JC, Peng D, Hua F, Li K, Yu JJ, Lv XX, Cui B, Liu SS, Yu JM, *et al*: Disrupting the TRIB3-SQSTM1 interaction reduces liver fibrosis by restoring autophagy and suppressing exosome-mediated HSC activation. Autophagy 16: 782-796, 2020.
37. Homewood CA, Warhurst DC, Peters W and Baggaley VC: Lysosomes, pH and the anti-malarial action of chloroquine. Nature 235: 50-52, 1972.
38. Qi X, Jiang L and Cao J: Senotherapies: A novel strategy for synergistic anti-tumor therapy. Drug Discov Today 27: 103365, 2022.
39. Cam H and Dynlacht BD: Emerging roles for E2F: beyond the G1/S transition and DNA replication. Cancer Cell 3: 311-316, 2003.
40. Ruscetti M, Morris JP IV, Mezzadra R, Russell J, Leibold J, Romesser PB, Simon J, Kulick A, Ho YJ, Fennell M, *et al*: Senescence-induced vascular remodeling creates therapeutic vulnerabilities in pancreas cancer. Cell 181: 424-441.e21, 2020.
41. Xiang J, Bandura J, Zhang P, Jin Y, Reuter H and Edgar BA: EGFR-dependent TOR-independent endocycles support *Drosophila* gut epithelial regeneration. Nat Commun 8: 15125, 2017.
42. Yu JJ, Zhou DD, Yang XX, Cui B, Tan FW, Wang J, Li K, Shang S, Zhang C, Lv XX, *et al*: TRIB3-EGFR interaction promotes lung cancer progression and defines a therapeutic target. Nat Commun 11: 3660, 2020.
43. Yu JM, Sun W, Wang ZH, Liang X, Hua F, Li K, Lv XX, Zhang XW, Liu YY, Yu JJ, *et al*: TRIB3 supports breast cancer stemness by suppressing FOXO1 degradation and enhancing SOX2 transcription. Nat Commun 10: 5720, 2019.

44. Li CM, Haratipour P, Lingeman RG, Perry JJP, Gu L, Hickey RJ and Malkas LH: Novel peptide therapeutic approaches for cancer treatment. Cells 10: 2908, 2021.
45. De Groot AS, Roberts BJ, Mattei A, Lelias S, Boyle C and Martin WD: Immunogenicity risk assessment of synthetic peptide drugs and their impurities. Drug Discov Today 28: 103714, 2023.
46. Settembre C, Di Malta C, Polito VA, Garcia Arencibia M, Vetrini F, Erdin S, Erdin SU, Huynh T, Medina D, Colella P, et al: TFEB links autophagy to lysosomal biogenesis. Science 332: 1429-1433, 2011.
47. Ferron M, Settembre C, Shimazu J, Lacombe J, Kato S, Rawlings DJ, Ballabio A and Karsenty G: A RANKL-PKCβ-TFEB signaling cascade is necessary for lysosomal biogenesis in osteoclasts. Genes Dev 27: 955-969, 2013.
48. Yin Q, Jian Y, Xu M, Huang X, Wang N, Liu Z, Li Q, Li J, Zhou H, Xu L, et al: CDK4/6 regulate lysosome biogenesis through TFEB/TFE3. J Cell Biol 219: e201911036, 2020.
49. Lv XX, Zheng XY, Yu JJ, Ma HR, Hua C and Gao RT: EGFR enhances the stemness and progression of oral cancer through inhibiting autophagic degradation of SOX2. Cancer Med 9: 1131-1140, 2020.
50. Hu F, Li C, Zheng X, Zhang H, Shen Y, Zhou L, Yang X, Han B and Zhang X: Lung adenocarcinoma resistance to therapy with EGFR-tyrosine kinase inhibitors is related to increased expression of cancer stem cell markers SOX2, OCT4 and NANOG. Oncol Rep 43: 727-735, 2020.
51. Chou YT, Lee CC, Hsiao SH, Lin SE, Lin SC, Chung CH, Chung CH, Kao YR, Wang YH, Chen CT, et al: The emerging role of SOX2 in cell proliferation and survival and its cross-talk with oncogenic signaling in lung cancer. Stem Cells 31: 2607-2619, 2013.
52. Ellis P, Fagan BM, Magness ST, Hutton S, Taranova O, Hayashi S, McMahon A, Rao M and Pevny L: SOX2, a persistent marker for multipotential neural stem cells derived from embryonic stem cells, the embryo or the adult. Dev Neurosci 26: 148-165, 2004.
53. Garros-Regulez L, Garcia I, Carrasco-Garcia E, Lantero A, Aldaz P, Moreno-Cugnon L, Arrizabalaga O, Undabeitia J, Torres-Bayona S, Villanua J, et al: Targeting SOX2 as a therapeutic strategy in glioblastoma. Front Oncol 6: 222, 2016.
54. Zhang X, Lu F, Wang J, Yin F, Xu Z, Qi D, Wu X, Cao Y, Liang W, Liu Y, et al: Pluripotent stem cell protein Sox2 confers sensitivity to LSD1 inhibition in cancer cells. Cell Rep 5: 445-457, 2013.
55. Tang Z, Kang B, Li C, Chen T and Zhang Z: GEPIA2: An enhanced web server for large-scale expression profiling and interactive analysis. Nucleic Acids Res 47 (W1): W556-W560, 2019.